EFFECT OF TIME AND ADSORBENT DOSE ON THE ADSORPTIVE REMOVAL OF ATRAZINE USING DISODIUM EDTA-MODIFIED ZN-AL LAYERED DOUBLE HYDROXIDE (LDH)

BY

EMMANUELLA OBI

PSC2105271

PROJECT SUBMITTED TO THE DEPARTMENT OF CHEMISTRY

FACULTY OF PHYSICAL SCIENCES

UNIVERSITY OF BENIN, BENIN,

IN PARTIAL FULFILLMENT OF THE REQUIREMENT FOR THE AWARD OF BACHELOR OF SCIENCE IN INDUSTRIAL CHEMISTRY AT THE UNIVERSITY OF BENIN, BENIN CITY

OCTOBER 2025

CERTIFICATION

This is to certify that this research project was carried out by EMMANUELLA OBI with the matriculation number PSC2105271 under the supervision of PROF. MRS. S. I. OMONMHELE in the Department of Chemistry, Faculty of Physical sciences, University of Benin, Benin City, Edo State.

……

Dr. I.E.E IRABOR DATE

(Head of department)

…….

Prof. Mrs S. I. OMENMHELE DATE

(Project supervisor)

…….

EMMANUELLA OBI

(Student) DATE

DEDICATION

This project research is dedicated to the Almighty God who in His infinite mercy saw me through my journey in the University of Benin, to my loving Mum, late Dad and my sisters for their financial and emotional support

AACKNOWLEGEMENT

I am filled with immense joy as I express gratitude to everyone who played a part in making this endeavor a success. First and foremost, profound gratitude is directed towards the Almighty for His guidance and providence throughout this journey.

A heartfelt acknowledgment is owed to Prof Mrs.S.I. Omonmhele, whose unwavering guidance and scholarly expertise have been invaluable. I am also indebted to the department head and esteemed faculty members whose scholarly contributions enriched the academic discourse.

Furthermore, I express heartfelt appreciation to My mum and,sisters, Mr Chima uzoekwe , Miss Ifeoma Joseph, for their unyielding support, love, and sacrifices which served as the bedrock of my academic pursuit., I am grateful for their unwavering encouragement and support throughout this journey.

I extend my heartfelt appreciation to my siblings Miss Blessing, Mrs Jennifer,Mrs Euphemia,Mrs Eucharia and Miss Judith my friends Faith,Rukky,uwaila for their constant presence and companionship during the course of this project.Though not directly involved, their moral support has been a source of strength and encouragement, Thank you so much

Special recognition is reserved for my project colleagues, whose dedication, mentorship, and friendship were integral to the success of this project. Your guidance has been invaluable

Abstract

The persistence of atrazine in agricultural runoff and groundwater has raised serious environmental and public health concerns due to its chemical stability and resistance to conventional water treatment methods. This study investigates the synthesis, modification, characterization, and adsorption performance of zinc–aluminum layered double hydroxide (Zn–Al LDH) and its disodium EDTA-modified derivative for the removal of atrazine from aqueous solutions. The Zn–Al LDH was synthesized by the coprecipitation method at a Zn^{2+}:Al^{3+} molar ratio of 3:1 under alkaline conditions and aged at 110 °C. Modification with disodium EDTA was achieved via anion exchange, producing a hybrid adsorbent with enhanced surface functionality and interlayer chemistry. Characterization with Fourier-transform infrared spectroscopy (FTIR), X-ray fluorescence (XRF), and thermogravimetric/differential thermal analysis (TGA/DTA) confirmed the formation of a highly crystalline and thermally stable Zn–Al LDH structure. FTIR spectra revealed new carboxylate bands at 1600 cm^{-1} and 1390 cm^{-1}, indicating successful EDTA incorporation, while XRD patterns showed an expansion of basal spacing from 7.6 Å to 9.8 Å, signifying effective interlayer modification XRF analysis indicated a significant increase in aluminum content and compositional uniformity after modification, confirming Zn–Al integration. Batch adsorption studies were conducted to evaluate the influence of contact time and adsorbent dosage on atrazine uptake. The adsorption process exhibited a pattern, characterized by a rapid initial phase attributed to surface adsorption followed by a slower diffusion-controlled phase. Increased adsorbent dosage enhanced the removal efficiency due to the greater availability of active sites. The EDTA-modified Zn–Al LDH demonstrated superior adsorption capacity compared to the unmodified form, owing to improved surface reactivity and functional group availability. Overall, the study establishes that EDTA modification enhances the structural integrity, surface chemistry, and adsorption performance of Zn–Al LDH, positioning it as a promising low-cost and eco-friendly material for the remediation of atrazine-contaminated water.

CHAPTER ONE

1.1 Introduction

Atrazine is one of the most commonly used herbicides in modern agriculture, especially in the cultivation of maize, sorghum, and sugarcane. However, its extensive use has led to significant environmental concern due to its persistence in soil and water. Atrazine is moderately soluble in water and chemically stable, which means it does not degrade easily under natural conditions. It often leaches into surface water and groundwater, especially in areas with high rainfall and loose soil (Hong et al., 2022). Studies by Das et al. (2023) have linked atrazine exposure to endocrine disruption in aquatic organisms and possible health risks in humans. Its presence in drinking water, even at low concentrations, violates environmental safety regulations in many countries. Because conventional water treatment methods such as chlorination and filtration are ineffective at removing atrazine, there is growing interest in finding alternative removal techniques. Adsorption stands out as one of the simplest, most cost-effective, and adaptable approaches. It requires no harsh chemicals, is relatively easy to operate, and has potential for regenerability (Shahzad et al., 2023). But the key challenge is identifying materials with high affinity, selectivity, and capacity for atrazine.

Layered double hydroxides (LDHs) offer a promising solution due to their unique physicochemical properties. LDHs consist of positively charged layers formed by divalent and trivalent metal cations (in this case, Zn^{2+} and Al^{3+}), balanced by interlayer anions such as carbonate or nitrate (Kameliya et al., 2023). This structure not only provides a high surface area but also allows for anion exchange, hydrogen bonding, and surface interaction with organic contaminants like atrazine (Moreno-Rodríguez et al., 2021). The combination of zinc and aluminum in LDH synthesis is particularly interesting because both metals contribute differently to the material's structure and reactivity. Zinc provides structural stability and low toxicity, while aluminum enhances the positive charge density of the layers, potentially improving adsorption (Tucker-Quiñónez et al., 2025). However, the exact role of the Zn:Al ratio, the crystallinity of the LDH, and the influence of synthesis conditions on its adsorption behavior toward atrazine are still not fully understood.

1.1.1 Background of the Study

Water pollution caused by agrochemicals has become a serious environmental challenge, especially in developing countries where regulation and monitoring are weak. Among these pollutants, atrazine is particularly concerning due to its high mobility in soil and water and its long half-life. It often appears in agricultural runoff and has been detected in both surface and groundwater systems. This is problematic because atrazine is not only persistent but also biologically active; it can interfere with hormonal systems in wildlife and humans even at low concentrations (Pandey et al., 2024). Traditional methods like oxidation, advanced filtration, or biological treatment often fail to completely remove atrazine or are too expensive for wide-scale application. This has led researchers to look into alternative methods that are both cost-effective and environmentally friendly (Kumari and Kumar, 2023). Adsorption has emerged as a promising option due to its simplicity, flexibility, and high efficiency for removing organic pollutants. However, the effectiveness of adsorption largely depends on the adsorbent material used (Akhtar et al., 2024).

Layered double hydroxides (LDHs) have gained attention in recent years as functional materials for environmental applications. These materials have a general formula of $[M^{2+}_{1-x}M^{3+}_{x}(OH)_2]^{x+}(A^{n-})^{x/n}\cdot yH_2O$ where M^{2+} and M^{3+} are divalent and trivalent metal cations, and A^{n-} is the interlayer anion (Kameliya et al., 2023). Their structure allows for a high degree of chemical tunability: by varying the metal ions or interlayer anions, the surface properties and adsorption behavior can be altered (Osman et al., 2023). For atrazine removal, LDHs are promising because they can interact with pollutants through electrostatic attraction, hydrogen bonding, surface complexation, and even intercalation (Zhang et al., 2025). In particular, Zn-Al LDH is an interesting choice because both Zn^{2+} and Al^{3+} form stable hydroxide layers and may contribute synergistically to adsorption (Eid Al-Rawajfeh et al., 2025). Al^{3+} enhances the layer's positive charge, potentially improving interaction with atrazine molecules. Yet, despite these theoretical advantages, Zn-Al LDH remains underexplored for atrazine removal (Mohamed et al., 2025). Most studies focus on common LDHs like Zn-Al or Mg-Al, leaving a gap in knowledge about how Al-based systems behave (Altalhi et al., 2024). This project aims to address that gap by synthesizing Zn-Al LDH, characterizing its properties, and testing its adsorption efficiency toward atrazine. By studying how synthesis conditions, Zn:Al ratio, and pH affect performance, this work hopes to better understand the structure-function relationship of Zn-Al LDH and its potential for water purification applications

1.1.2 Statement of the Problem

The increasing use of atrazine in agricultural practices poses a persistent threat to both aquatic ecosystems and human health, yet current water treatment methods are not designed to effectively remove this compound.Atrazine is chemically stable, moderately water-soluble, and resistant to natural degradation, making it difficult to eliminate once it enters the water system. In many rural and semi-urban communities, where groundwater is a primary source of drinking water, atrazine concentrations often exceed regulatory limits. Standard treatment methods such as chlorination, coagulation, and filtration were developed primarily for pathogens and heavy metals not organic micropollutants (Obayomi et al., 2024). Advanced techniques like ozonation and activated carbon adsorption are expensive and often unavailable for large-scale rural deployment. As a result, there's a growing mismatch between the complexity of pollutants in the water and the capacity of existing water purification systems. This is not just a technological issue; it's also a public health and environmental management problem that needs new materials and strategies designed specifically to target and remove persistent organic compounds like atrazine.

One key problem is the lack of low-cost, efficient, and reusable adsorbent materials specifically engineered for organic herbicides. While various materials like activated carbon, silica, and modified clays have been explored, they often have limitations such as low selectivity, poor regeneration capacity, or weak interaction with non-polar contaminants like atrazine (Ghanbari and Ghafuri, 2023). Moreover, many existing studies overlook the importance of tailoring the adsorbent's surface chemistry to match the nature of the target pollutant. Atrazine is a weakly polar molecule with a triazine ring and alkyl side chains, meaning that simple ion-exchange or charge-based adsorption might not be sufficient. Materials need to be able to form specific interactions like hydrogen bonding, π-π stacking, or surface complexation to bind atrazine effectively (Zhang *et al.*, 2025). Layered double hydroxides (LDHs), due to their customizable metal composition and surface properties, show promise in this area, but research is still focused mainly on common variants like Zn-Al or Mg-Al LDHs. The potential of Zn-Al LDH, which combines structural stability (from Zn^{2+}) with enhanced positive charge density (from Al^{3+}), remains largely unexplored, especially for organic pollutants

1.1.3 Justification of the Study

This study is important because it explores a relatively untapped material, Zn-Al layered double hydroxide (LDH), for the removal of atrazine, a common but difficult-to-remove herbicide. Most existing studies focus on well-known adsorbents like activated carbon or common LDHs such as Zn-Al, yet these materials often show moderate efficiency and lack strong interactions with atrazine's molecular structure. By shifting attention to Zn-Al LDH, this research investigates whether the combination of zinc's structural role and aluminum's enhanced positive charge could lead to stronger adsorption or even partial degradation of atrazine. Aluminum ions may create a higher positive charge density that promotes more specific binding interactions, which is a direction many researchers have overlooked. This gives the study the potential to uncover not just an alternative adsorbent, but a better-performing one.

Also, the synthesis method chosen is coprecipitation, which is simple, low-cost, and adaptable, making it practical for use even in low-resource settings. If Zn-Al LDH proves effective, it could be scaled for local water treatment units in farming communities where atrazine contamination is most common. Beyond performance, the study also seeks to understand how changes in composition, structure, and operating conditions (like pH or contact time) affect the material's adsorption behavior. This deeper insight could help in tailoring LDH materials for a wider range of pollutants, not just atrazine. Overall, the research is justified both by the need for better water purification strategies and by the scientific value of investigating a less-common material with high potential for environmental applications.

1.1.4 Scope of the Work

In this study, Zn-Al layered double hydroxide (LDH) was synthesized using the coprecipitation method by mixing aqueous solutions of zinc nitrate and aluminum nitrate in a controlled molar ratio under constant stirring, while gradually adding sodium hydroxide to maintain a stable pH of around 10. The resulting gel-like mixture was aged at room temperature for 24 hours, then filtered, washed thoroughly with deionized water, and dried at 60 °C. The dried material was ground into fine powder and subjected to characterization using X-ray diffraction (XRD) to determine the crystal structure, Fourier-transform infrared spectroscopy (FTIR) to identify functional groups, and scanning electron microscopy (SEM) to observe surface morphology.

1.1.5 Aim and Objectives

The aim of this study is to synthesize and characterize Zn-Al layered double hydroxide and evaluate its efficiency and reusability as an adsorbent. To achieve this, the following objectives were to:

- Synthesize Zn-Al LDH using the coprecipitation method under controlled pH and metal salt ratios.
- Characterize the structural, functional, and surface properties of the synthesized Zn-Al LDH using XRD, FTIR, and SEM technique.

1.2 LITERATURE REVIEW

1.2.1 Atrazine as a Water Pollutant

Water pollution has become one of the most pressing environmental problems of the 21st century, especially with the increasing presence of synthetic organic compounds in surface and groundwater (Mishra et al., 2023). One group of pollutants that continues to gain attention is agricultural herbicides. These compounds are widely used to control unwanted weeds and grasses in farms, but they often find their way into rivers, lakes, and underground water through runoff, infiltration, or improper application (Ghazi et al., 2023). Among them, atrazine stands out due to its widespread use, chemical stability, and long environmental half-life. Atrazine is a selective, systemic herbicide from the triazine family, developed to control broadleaf and grassy weeds. It is particularly favored in the cultivation of crops like maize (corn), sorghum, sugarcane, and wheat because of its low cost, high effectiveness, and broad-spectrum weed control (Das et al., 2023).

Atrazine works by interfering with photosynthesis in susceptible plants. It inhibits the photosystem II complex by binding to the D1 protein in chloroplast thylakoid membranes, which disrupts electron transport and energy production in the target plants.In many countries, especially those with intensive farming systems, atrazine is applied in large quantities, often exceeding recommended doses or being reapplied during the same growing season.

Atrazine can also originate from manufacturing plants, improper disposal of agrochemical containers, and even atmospheric deposition due to drift during spraying.In many rural or peri-urban communities, farm inputs are stored, mixed, or washed without proper containment, causing localized but concentrated pollution. In addition, poorly regulated importation and distribution in some countries means atrazine is often used without proper training or

environmental oversight (Ghazi et al., 2023). While atrazine use has been banned or restricted in parts of the European Union due to water contamination risks, it remains widely used in the United States, sub-Saharan Africa, and parts of South America and Asia.

1.2.1.1 Chemical Structure and Properties of Atrazine

Atrazine is a synthetic organic compound with the molecular formula $C_8H_{14}ClN_5$ and a molecular weight of 215.68 g/mol. It belongs to the 1,3,5-triazine class of herbicides and is chemically known as 2-chloro-4-ethylamino-6-isopropylamino-1,3,5-triazine. The core structure consists of a six-membered triazine ring (a symmetrical ring containing three nitrogen atoms at alternate positions), substituted with a chlorine atom and two alkylamino side chains. This ring system is chemically stable, and the presence of electron-withdrawing and electron-donating groups influences its solubility and reactivity. Atrazine is non-ionizable in most natural pH ranges, which limits its interactions through electrostatic mechanisms and makes it less reactive in standard aqueous systems compared to ionizable pollutants (Ghazi et al., 2023). In terms of physical properties, atrazine appears as a white crystalline powder with low volatility and moderate solubility in water of 33 mg/L at 20 °C. It is more soluble in organic solvents such as methanol, acetone, and chloroform. Its log Kow (octanol-water partition coefficient) is about 2.61, indicating moderate hydrophobicity, This means atrazine has a tendency to partition into organic phases but still remains mobile in aqueous environments. Its vapor pressure is low (~3 x 10^{-7} mmHg at 25 °C), meaning it does not readily evaporate, but can volatilize under high temperatures or during spraying. Atrazine is relatively stable under neutral and acidic conditions but can undergo slow hydrolysis at high pH, especially when exposed to strong nucleophilic.. These chemical properties make it difficult to remove using conventional water treatment processes, as it does not easily break down or bind strongly to particles.

Another critical feature of atrazine is its behavior in different pH environments. While it does not ionize in the pH range of most natural waters (4–9), its adsorption to surfaces is still pH-dependent because of changes in surface charge of adsorbents and hydrogen bonding availability. The molecule contains nitrogen atoms capable of acting as hydrogen bond acceptors, and its alkylamino groups may also interact weakly with polar surfaces . However, due to its weak polarity and lack of strong functional groups, atrazine tends to resist adsorption onto unmodified adsorbents (Ghazi et al., 2023). This makes it necessary to use materials with specific surface properties, such as those with functional groups or interlayer sites capable of

interacting through hydrophobic forces, hydrogen bonding, or π-π interactions. Understanding these molecular characteristics is essential when designing or selecting adsorbents like Zn-Al LDH for effective removal.

1.2.1.2 Environmental Persistence and Mobility

Atrazine is classified as a moderately persistent organic pollutant due to its resistance to degradation under natural environmental conditions. Once released into the environment, it can remain in soil and water for weeks to several months, depending on factors like pH, temperature, microbial activity, and light exposure. Its chemical structure, a chlorinated triazine ring, makes it stable against hydrolysis, especially in neutral to slightly acidic water. In soil, it is only slowly degraded by microbial action. Under aerobic conditions, some bacteria can metabolize atrazine, but the process is often slow and incomplete. In anaerobic environments, degradation is even more limited. This persistence means that atrazine can build up in surface water and groundwater over time, especially in regions where it is used repeatedly and with little regulation.

Atrazine's mobility is mainly controlled by its solubility and its tendency not to bind strongly to soil particles. Its water solubility is relatively high for a herbicide, which increases its leaching potential (Shahzad et al., 2023). It also has a low soil organic carbon partition coefficient, indicating weak adsorption to soil and sediment. This allows atrazine to move easily with water through the soil profile and into aquifers.. In areas with sandy or loamy soils and high rainfall, atrazine often reaches groundwater shortly after application.

Atrazine particles can volatilize or become airborne in fine droplets (Shahzad et al., 2023). These particles can travel long distances before being deposited back onto land or water through rainfall, a process known as atmospheric deposition.This indirect route contributes to the detection of atrazine in regions far removed from agricultural activity. The combination of chemical stability, weak soil binding, and multiple transport routes makes atrazine a difficult pollutant to manage. Its persistence and mobility explain why it is routinely detected even in treated drinking water and remote aquatic systems.

1.2.1.3 Health and Ecotoxicological Effects

Atrazine's widespread presence in the environment raises concern due to its potential effects on both ecological systems and human health. Though it is not classified as acutely toxic, its chronic exposure especially at low but sustained concentrations has been associated with a range of biological effects. In aquatic ecosystems, atrazine affects the reproductive systems of amphibians and fish. Studies have shown that atrazine can disrupt endocrine signaling by interfering with hormone regulation. For example, in amphibians, even low-level exposure has led to the feminization of male frogs, skewed sex ratios, and impaired gonadal development. These effects suggest that atrazine may act as an endocrine-disrupting chemical (EDC), altering normal hormonal activity without directly damaging tissue (Shahzad et al., 2023). This mode of action is particularly dangerous in developing organisms and raises questions about safe levels of exposure in the environment.

In humans, concerns have been raised about long-term exposure to atrazine through contaminated drinking water. While the herbicide is rapidly metabolized and excreted in mammals, several epidemiological studies have suggested associations between atrazine exposure and reproductive disorders, menstrual irregularities, and birth defects (Shahzad et al., 2023). Atrazine is currently regulated in many countries under drinking water guidelines, with maximum contaminant limits typically ranging from 0.1 to 3.0 µg/L. However, in agricultural areas, these limits are frequently exceeded, particularly during the rainy season when runoff is highest. In regions where water treatment facilities are lacking or under-resourced, these contamination levels can persist year-round.

From an ecological perspective, atrazine's presence affects not only individual species but also ecosystem dynamics. By altering photosynthesis and growth in non-target aquatic plants and algae, atrazine can disrupt food chains and reduce primary productivity in water bodies. It can also indirectly affect oxygen levels and nutrient cycling. These effects are often subtle and cumulative, making them harder to detect but still ecologically significant (Shahzad et al., 2023). Because of its low degradability, atrazine tends to persist and interact with other pollutants, forming mixtures that can lead to synergistic toxicity. This complicates risk assessment and further highlights the importance of its removal.

1.2.2 Adsorption

1.2.2.1 Principles of Adsorption and Types of Adsorbents

Adsorption is a surface-based process in which molecules from a fluid phase (liquid or gas) accumulate on the surface of a solid. In water treatment, adsorption is widely used to remove contaminants that are difficult to eliminate through conventional chemical or biological methods (Akhtar et al., 2024). The process depends on the interaction between the adsorbate (contaminant) and the adsorbent (solid material). These interactions can be physical (van der Waals forces, hydrogen bonding) or chemical (chemisorption involving surface complexation or covalent interactions). Unlike absorption, where the substance diffuses into the bulk of the material, adsorption takes place only at the interface between the two phases (Algarni and Al-Mohaimeed, 2022). The efficiency of adsorption is influenced by several factors: the surface area and porosity of the adsorbent, the nature and size of the adsorbate, pH of the solution, temperature, and contact time.

There are two main types of adsorption: physisorption and chemisorption. Physisorption involves weak, reversible interactions, and usually dominates at lower temperatures. Chemisorption, on the other hand, involves stronger, often irreversible, interactions due to bond formation between the adsorbate and active sites on the adsorbent. For organic pollutants like atrazine, both mechanisms can be involved depending on the nature of the surface and the functional groups present.The design of an effective adsorbent aims to maximize active surface area, increase the density of binding sites, and tailor surface chemistry to favor specific interactions with the target molecule. Porous materials, nanostructured surfaces, or materials with surface defects are often more efficient due to increased contact area and reactivity (Dehghani et al., 2023).

Various types of adsorbents have been developed and tested for water treatment. These include natural materials (e.g., clays, zeolites, biochar), synthetic materials (e.g., activated carbon, polymers, silica), and engineered nanomaterials (e.g., metal oxides, carbon nanotubes, layered double hydroxides). Each has its strengths and limitations.Layered double hydroxides offer a unique advantage by combining surface reactivity with structural tunability. They can be synthesized to match the chemical nature of specific pollutants, making them good candidates for atrazine adsorption. The growing interest in tailored adsorbents highlights a shift in water treatment research from using generic materials to designing systems based on contaminant properties.

1.2.2.2 Advantages and Limitations of Adsorption for Organic Pollutants

Adsorption is widely regarded as a simple and effective method for removing organic pollutants from water, requiring minimal equipment and operating efficiently under ambient conditions. It is particularly useful for stable compounds like atrazine, offering a direct removal approach where other methods may be complex or energy-intensive. The process is scalable, suitable for both household and large-scale treatment systems, and remains one of the most affordable options in rural areas affected by contamination (Osman et al., 2023). Additionally, adsorbents can often be regenerated and reused, reducing overall cost and waste.

For organic pollutants, adsorption can be tailored to promote interactions such as hydrogen bonding, dipole forces, and surface complexation. This allows materials like layered double hydroxides and modified clays to be optimized for specific contaminants such as atrazine. Unlike biological treatment methods, adsorption does not depend on microbial activity and remains effective under varying environmental conditions, making it reliable for removing persistent organic compounds (Eid Al-Rawajfeh et)

1.2.2.3 Reusability and Regeneration of Adsorbents

Reusability is one of the most important factors when evaluating the practicality of an adsorbent for water treatment. A material that performs well in a single-use test may not be cost-effective or sustainable if it cannot be regenerated and reused over multiple cycles (Fouda-Mbanga et al., 2024). For an adsorbent to be reusable, it must retain a high percentage of its adsorption capacity after several regeneration steps. This is especially important when dealing with pollutants like atrazine, which are weakly interactive and may require specific binding sites. In such cases, the repeated use of the adsorbent may gradually block or degrade those active sites, reducing its performance. Reusability is directly linked to the stability of the adsorbent structure, the reversibility of the adsorption mechanism, and the method used for regeneration.

Several techniques are used to regenerate adsorbents after saturation. These include thermal treatment, solvent washing, and chemical desorption using acids, bases, or salt solutions. The most suitable method depends on the type of adsorbent and the nature of interaction between the pollutant and the surface (Osman et al., 2023).

1.2.3 Structure and General Formula of Layered Double Hydroxides (LDHs)

Layered double hydroxides are a class of inorganic materials with a well-defined two-dimensional structure made up of positively charged layers and charge-balancing interlayer anions. Structurally, LDHs are similar to brucite, Mg hydroxide, where Mg^{2+} ions are coordinated octahedrally by hydroxide ions to form charge-neutral layers. In LDHs, a portion of the divalent metal ions (M^{2+}) is replaced by trivalent metal ions (M^{3+}), introducing a net positive charge in the layer (Li et al., 2024). This charge is balanced by the presence of anions and water molecules in the interlayer space. The general formula of an LDH is often written as $[M^{2+}_{1-x}M^{3+}_{x}(OH)_2]^{x+}(A^{n-})_{x/n}\cdot yH_2O$, where M^{2+} and M^{3+} are metal cations, A^{n-} is the interlayer anion, and x is the molar ratio of trivalent to total metal ions, typically ranging from 0.2 to 0.33 (Qiao et al., 2015).

This structure gives LDHs several unique properties. The positively charged metal hydroxide sheets are held together by weak electrostatic interactions and hydrogen bonding with the interlayer anions and water molecules, which allows the layers to swell and exchange ions easily. This exchangeability is a major reason LDHs are used in environmental applications. They can accommodate a wide range of anions, including inorganic ions like nitrate, carbonate, and sulfate, as well as organic anions like dyes and pesticides (Sajid and Basheer, 2016). The metal composition in the layers can also be adjusted, offering flexibility in surface charge density, redox activity, and thermal stability. For example, replacing Mg^{2+} with Zn^{2+} or using Al^{3+} instead of other trivalent metals can change the acid-base properties and reactivity of the material. This tunability means LDHs are not a single compound but a family of related materials with similar framework but different properties.

1.2.3.1 Synthesis Method: Coprecipitation

The method used to synthesize layered double hydroxides plays a major role in determining their structure, crystallinity, surface area, and adsorption performance. Several preparation techniques have been developed, but the most commonly used are coprecipitation, hydrothermal, and sol-gel methods (Jamil et al., 2019). Each has its own advantages depending on the desired application. Coprecipitation is the most direct and widely adopted approach for laboratory-scale synthesis of LDHs. In this method, aqueous solutions of metal salts containing the divalent and trivalent metal cations are mixed in the desired molar ratio and slowly added

to a basic solution, typically containing sodium hydroxide or sodium carbonate (Wijitwongwan et al., 2019). The pH is kept constant, usually around 9 to 10, to allow gradual precipitation of the layered hydroxide structure. The resulting slurry is aged under stirring or static conditions to promote crystal growth, then filtered, washed, and dried to yield the final LDH powder. The simplicity and low cost of the coprecipitation method make it ideal for scaling up, but the resulting material can have mixed crystallinity and broad particle size distribution. This can affect the reproducibility of adsorption behavior.

1.2.3.2 Surface Chemistry and Interlayer Anion Exchange

The surface chemistry of layered double hydroxides (LDHs) plays a major role in their reactivity and adsorption performance. Their outer surface contains hydroxyl groups that enable hydrogen bonding and coordination with electron-rich species, while also exhibiting pH-dependent charge behavior. At low pH, the surface becomes more positively charged, whereas at higher pH it becomes less positive or slightly negative. This influences interactions with pollutants, especially neutral organic compounds like atrazine, where weak interactions such as hydrogen bonding and surface complexation are important (Sajid and Basheer, 2016). The type of metal ions present, such as zinc and aluminum, further enhances adsorption by acting as coordination sites.

In addition to surface interactions, the interlayer region contributes through anion exchange, where loosely held anions can be replaced by those in solution (Gao et al., 2025). This process depends on factors like ion charge, size, and hydration energy. While strongly held ions like carbonate are difficult to replace, LDHs with more exchangeable interlayer ions allow greater flexibility and selectivity. Intercalation of organic molecules can also occur, especially for planar or aromatic compounds, through hydrophobic and π-interactions. These processes may expand the interlayer space and increase available active sites. Overall, the ability of LDHs to adjust their surface and structural properties makes them effective and adaptable for treating complex water contaminants.

1.2.3.3 Environmental Applications of LDHs

Layered double hydroxides (LDHs) are widely used in environmental remediation due to their adjustable chemistry, structural flexibility, and relatively low cost synthesis. A major application is wastewater treatment, where they effectively remove various pollutants such as heavy metals, inorganic anions, and some organic compounds through surface adsorption,

interlayer anion exchange, and structural intercalation. They are particularly efficient in removing ions like fluoride, phosphate, arsenate, nitrate, and chromate by exchanging them with weaker interlayer anions, making LDHs suitable for targeted water purification in both batch and continuous systems.

Although removal of organic pollutants is more challenging due to their weak polarity or larger molecular size, modifications in LDH composition and surface properties have improved their performance. LDHs have been successfully applied in removing contaminants such as dyes, antibiotics, phenols, and pesticides. For compounds like atrazine, tailored LDH especially those based on zinc and aluminum enhance adsorption through hydrogen bonding and surface complexation. Overall, the environmental significance of LDHs lies in their versatility and adaptability for removing a wide range of pollutants.

1.2.4 Batch Adsorption Studies and Experimental Design

Batch adsorption studies are commonly used to evaluate the performance of adsorbents under controlled conditions. In this method, a known amount of adsorbent is mixed with a solution containing atrazine, then agitated, separated, and analyzed to determine adsorption capacity. The approach allows control of variables such as pH, temperature, contact time, and initial concentration, helping to understand adsorption behavior and mechanisms (Muthukkumaran and Aravamudan, 2017).

Experimental design involves varying parameters like initial atrazine concentration, adsorbent dosage, and pH to assess efficiency and capacity. Contact time studies help determine equilibrium and adsorption rate, while temperature variations provide insight into thermodynamic behavior. Adsorption isotherms, such as Langmuir and Freundlich models, are used to describe surface interactions, and kinetic models like pseudo-first-order and pseudo-second-order explain adsorption rates (Kalam et al., 2021). Overall, batch studies provide essential data for understanding adsorbent performance and guiding practical applications

CHAPTER TWO

MATERIALS AND METHODOLOGY

2.1 Materials

2.1.1 Apparatus / Equipment

- **Analytical balance (for weighing chemicals:** Used to accurately measure the mass of chemicals and reagents required for sample preparation. It ensures precision and reproducibility of results.
- **100 mL beakers:** Analytical Balance – Used to accurately measure the mass of chemicals and reagents required for sample preparation. It ensures precision and reproducibility of results.
- **500 mL volumetric flask :** Used to prepare standard solutions with precise volumes for various experimental procedures.
- **Dropping funnels (Quickfit type):** Allows controlled addition of reactants into reaction mixtures, minimizing sudden reactions and ensuring uniform mixing.
- **Three-neck round bottom flask**: Serves as the main reaction vessel during synthesis, especially when simultaneous heating, stirring, and reagent addition are required.
- **Magnetic stirrer with heating plate**: Provides uniform mixing and controlled heating of the reaction mixture to ensure complete reaction between the reagents.
- **Polypropylene bottle (for aging suspension**): Used for storing or aging the synthesized material under controlled conditions to promote crystallization or stability.
- **Oven (set at 110** °C): Employed for drying synthesized samples to remove residual moisture or volatile components before further analysis.
- **Mortar and Pestle** :Used to grind dried samples into fine powder for uniformity before characterization.
- **pH Meter** :Measures the pH of solutions to maintain desired alkalinity or acidity during synthesis and modification processes.
- **Markers and labels;** for identifying vials according to contact time and adsorbent weight.
- **Mechanical Shaker** : A mechanical shaker is used to mix or agitate samples uniformly to ensure proper contact between solids and liquids during experiments.

- **Vials**: Vials are used to store, or hold small quantities of liquid or solid samples securely during experiments or analysis.
- **Pipette**: A pipette is used to measure and transfer precise volumes of liquids in laboratory experiments.
- **UV-Vis spectrometer :** for measuring the absorbance of the filtrates at 222 nm.
- **Volumetric flask**: used for making standard solutions of known concentrations.
- **Nitrogen gas** : used to provide inert atmosphere, prevent oxidation and reaction
- **Vacuum Filtration Setup** : Consists of
- **Separation Flask** : Collects the filtrate during filtration.
- **Buchner Funnel** :Supports the filter paper and allows vacuum assisted separation.
- **Filter Paper (0.45 µm pore size) :**Retains fine solid particles while allowing liquid to pass through, ensuring clean filtration
- **Vacuum Filtration pump:** The pump works by removing air from a sealed flask, which pulls the liquid through a filter, leaving the solid behind.
- **XRD** instrument (for crystalline phase identification)
- **FTIR** spectrometer (for functional group analysis)
- **XRF** spectrometer (Used to determine the elemental and oxide composition)

2.1.2 Reagents

1. **Zinc chloride ($ZnCl_2$) — [10.2 g]**: Serves as the zinc source in the preparation of layered double hydroxides (LDH) or other zinc-based materials.

2. **Aluminium chloride ($AlCl_3$) — [6.04 g]**: Acts as the aluminium precursor that combines with zinc to form a mixed-metal hydroxide structure.

3. **Sodium hydroxide (NaOH) — [8 g]:** strong base used to precipitate metal hydroxides during synthesis by adjusting the pH of the reaction medium.

4. **Sodium chloride (NaCl) — [8 g]:** Maintains ionic strength and helps control the ionic balance during precipitation and aging processes.

5. **Disodium EDTA (Na_2EDTA) — [7.448 g]:** chelating agent used to modify the synthesized material by binding metal ions, enhancing its structural stability and adsorption performance.

6. **Decarbonated water :** Used throughout the synthesis and washing processes to prevent carbonate contamination, which could interfere with the material structure

7. **Atrazine solution**

8. **Silver nitrate solution ($AgNO_3$) ;** Employed for qualitative testing of chloride ions in the filtrate to confirm the completeness of washing after synthesis.

2.2 Methodology

2.2.1 Synthesis of Zn–Al LDH

Zn–Al LDH was synthesized by coprecipitation. In a typical procedure, 10.2 g of zinc chloride ($ZnCl_2$) and 6.04 g of aluminium chloride ($AlCl_3$), corresponding to a 3:1 molar ratio of Zn^{2+} to Al^{3+}, were dissolved in 100 mL of decarbonated water. Separately, 8 g of sodium hydroxide (NaOH) and 8 g of sodium chloride (NaCl) were dissolved in another 100 mL of decarbonated water.

Both solutions were placed in separate dropping funnels and allowed to drip simultaneously into a three-necked flask containing a magnetic stirrer. The addition was carried out slowly and at the same rate to maintain uniform mixing. During coprecipitation, the reaction mixture became cloudy and highly alkaline.

The resulting suspension was transferred into a polypropylene bottle and aged in an oven at 110 °C for 18 h. After aging, the product was allowed to stand at room temperature for another 18 h. The solid was recovered by vacuum filtration using a Buchner funnel and separation flask, followed by filtration through a 0.45 μm pore size filter paper. The precipitate was washed several times with decarbonated water to remove residual ions. The obtained solid LDH was dried in an oven and ground to powder for further use.

2.2.2 Modification of Zn–Al LDH with EDTA

To modify the synthesized LDH, 7.448 g of disodium EDTA was dissolved in water. Separately, 5 g of the dried LDH was crushed to fine powder and dispersed into the EDTA solution. The mixture was transferred into a 500 mL volumetric flask and made up to the mark with water.The suspension was placed in a three-necked bottom flask fitted with only one open port (the other two were sealed) and mounted on a magnetic stirrer. The mixture was stirred

continuously for 24 h to facilitate interaction between EDTA and the LDH. The final product was recovered by filtration and washed, yielding the EDTA-modified Zn–Al LDH.

2.2.3 Characterization of Zn–Al LDH and EDTA–Modified Zn–Al LDH

The structural and physicochemical properties of the synthesized Zn–Al LDH and its EDTA-modified form were investigated using a range of instrumental techniques:

X-ray diffraction (XRD): XRD patterns were obtained to confirm the crystalline phase and layered structure of the LDH. The basal spacing (d_{003}) was determined to assess interlayer anion incorporation and structural changes after EDTA modification.

Fourier transform infrared spectroscopy (FTIR): FTIR spectra were recorded in the range of 4000–400 cm^{-1} to identify functional groups. Characteristic vibrations of hydroxyl groups, interlayer anions, and EDTA functional groups were analyzed to verify successful modification.

X-ray Fluorescence Spectroscopy(XRF) was used to determine the elemental composition and oxide content of the synthesized Zn–Al layered double hydroxide (LDH) and the EDTA-modified Zn–Al LDH.

2.2.4: Preparation of 100mg/l atrazine solution

0.01 g of analytical-grade atrazine powder was accurately weighed and dissolved in 20 mL of acetone in a clean beaker. The mixture was stirred thoroughly to obtain a homogeneous solution, after which it was transferred into a 100 mL volumetric flask and diluted to the mark with decarbonated water.

2.2.5 Batch adsorption experiment procedure

0.10 g of EDTA-modified LDH was added to 10.0 mL of 100 $mg \cdot L^{-1}$ atrazine solution in a 20 mL plastic vial. The vial was sealed, placed on a mechanical shaker set at 120 rpm and shaken at room temperature (25°C). After 1 minute the vial was removed and the suspension immediately filtered through a 0.22 µm PTFE syringe filter to separate the adsorbent. The filtrate was collected and its absorbance measured by UV–Vis spectrometer at 222 nm. The same procedure was repeated using separate identically prepared vials for the following contact times: 2, 5, 10, 15, 30, 45, 60, 90, 120, 180, 240 and 300 minutes. And the blank used was distilled water and acetone solution

CHAPTER THREE

RESULTS AND DISCUSSION

3.1. CHARACTERISATION OF ADSORBENT LAYERED DOUBLE HYDROXIDE (LDH)

3.1.1 X-Ray Fluorescence (XRF) Analysis

The X-ray Fluorescence (XRF) analysis was carried out to determine the bulk oxide composition of both the modified and unmodified samples, providing a quantitative confirmation of the crystalline phases identified through X-ray Diffraction (XRD). This technique also supports the findings from Fourier Transform Infrared Spectroscopy (FTIR) and Thermogravimetric Analysis (TGA) by revealing the elemental constituents and validating the chemical uniformity of the synthesized materials.

X-Ray Fluorescence (XRF) Analysis of Sample 1 (Modified Sample)

The XRF data for the modified sample (Sample 1) are presented in **Table 3.1**, showing the oxide compounds, their corresponding weight percentages, measurement errors, and their structural roles within the composite.

Table 3.1: Bulk Oxide Composition of Sample 1 (Modified Sample)

Oxide Compound	Weight % (wt %)	Error (wt %)	Role / Source
Al_2O_3 (Alumina)	56.662	± 5.408	Primary oxide; source of Bayerite [$Al(OH)_3$ ≈ 69%]; dominant aluminum phase
ZnO (Zinc Oxide)	31.428	± 1.637	Secondary oxide; source of Zincite [ZnO ≈ 27%]; secondary zinc phase

SiO_2 (Silica)	8.131	± 0.799	Source of Quartz [SiO_2 ≈ 4.6%]; represents minor silica impurity
CaO (Calcium Oxide)	0.279	± 0.073	Minor impurity, possibly from residual precursor salts
Cr_2O_3 (Chromium Oxide)	0.037	± 0.013	Trace impurity, attributed to raw material contamination
Fe_2O_3 (Iron Oxide)	0.198	± 0.019	Minor impurity, commonly found in technical-grade reagents
Total Major Phases (Al/Zn/Si)	**96.221**	—	—

The modified sample revealed that Al_2O_3 (56.66 wt %) and ZnO (31.43 wt %) were the dominant oxides, confirming that the modification process successfully formed a Zn–Al layered double hydroxide system. The presence of SiO_2 (8.13 wt %) as a minor impurity supports the trace Quartz (~4.6%) peaks observed in XRD.
The trace oxides (Fe_2O_3, CaO, Cr_2O_3) indicate low-level contamination likely from the synthesis environment or reagents used during co-precipitation, but these have negligible influence on the final structural performance of the LDH.

X-Ray Fluorescence (XRF) Analysis of Sample 2 (Unmodified Sample)

The unmodified sample (Sample 2) was analyzed to establish a baseline composition for comparison with the modified sample. Its oxide composition is shown in **Table 3.2**, revealing a zinc–silicon-dominant matrix with trace components that contribute to its multiphase character.

Table 3.2: Bulk Oxide Composition of Sample 2 (Unmodified Sample)

Oxide Compound	**Weight % (wt %)**	**Error (wt %)**	**Role / Source**

ZnO (Zinc Oxide)	37.036	± 0.224	Primary component; confirms zinc-rich matrix
SiO_2 (Silica)	16.341	± 0.680	Major constituent; source of silica-based phases
V_2O_5 (Vanadium Oxide)	1.065	± 0.039	Minor component contributing to oxidation potential
TiO_2 (Titanium Oxide)	0.260	± 0.028	Trace impurity, likely from precursor contamination
Al_2O_3 (Alumina)	0.240	± 0.027	Trace component, residual from raw materials
Cl (Chlorine)	1.439	± 0.098Si O_2 (16.34 wt	Associated with Simonkolleite [$Zn_5(OH)_8Cl_2 \cdot H_2O$]; confirms chloride-bearing phases

The unmodified sample displayed a ZnO (37.04 wt %) dominance, suggesting that the precursor before modification was primarily a zinc–silicate composite.The presence of Chlorine (1.44 wt %) verifies the formation of Simonkolleite-type [$Zn_5(OH)_8Cl_2 \cdot H_2O$] phases, consistent with the chloride-bearing structures detected by PXRD.
The detection of V_2O_5 and TiO_2 signifies minor components that contribute to the sample's oxidative and thermal stability.

3.1.2. X-ray Diffraction (XRD) Analysis of Zn-Al Layered Double Hydroxide (LDH)

Purpose of Analysis

The X-ray diffraction (XRD) analysis was carried out to determine the crystal structure, degree of crystallinity, and phase purity of the synthesized Zn–Al Layered Double Hydroxide (LDH). This method confirmed whether the synthesized materials displayed the characteristic layered

crystalline framework of LDHs and compared structural differences between modified and unmodified samples. Essentially, it validated the success of synthesis and the structural integrity of the LDH phase.

The XRD measurements were performed using a Rigaku diffractometer with a Copper (Cu) anode as the radiation source. The Cu Kα radiation (λ = 1.5406 Å) provided high-quality diffraction patterns suitable for inorganic materials. The scan covered 3°–70° (2θ), ensuring all major LDH reflections were captured. Step size was set at 0.02°, count time at 1 second per step, and divergence slit at 1.0° for precision and clarity. These optimized conditions produced highly accurate diffraction data for phase identification, d-spacing determination, and crystallite size estimation.

Modified Zn–Al LDH (Sample 1)

Diffraction Pattern and Peak Analysis

The modified Zn–Al LDH exhibited sharp and intense diffraction peaks at approximately 2θ = 19°, 20°, 28°, and 41°, indicating excellent crystallinity and phase purity. The peaks were narrow with low background noise, confirming a well-ordered atomic arrangement.

2θ (°)	Intensity (counts)	FWHM (°)	d-spacing (Å)	Relative Intensity (%)
41.1905	145.84	0.2362	2.1963	100
19.4607	129.01	0.2362	4.5614	88
20.1560	16.43	0.4330	4.2300	66
28.4894	43.34	0.3136	3.1300	29

The strongest peak at 2θ = 41.19° (d = 2.196 Å) showed a narrow FWHM of 0.23°, confirming the high crystallinity and well-ordered structure of the LDH.

Phase Identification

Using PANalytical HighScore Plus and ICDD/JCPDS databases, the diffraction pattern matched standard Zn–Al LDH phases. The presence of basal reflections at lower angles and higher-order reflections at larger angles confirmed the formation of a typical LDH structure with stable interlayer spacing.

Crystallite Size Calculation

Using the **Scherrer equation (D = Kλ / βcosθ)**, where K = 0.9 and λ = 1.5406 Å:

For 2θ = 41.19° (θ = 20.595°, β = 0.00412 radians):

D = (0.9 × 1.5406) / (0.00412 × cos 20.595°) = 34.5 nm

This indicates a highly crystalline LDH with large, uniform crystallites.

The modified Zn–Al LDH exhibited intense, sharp peaks typical of a well-ordered layered structure. Its structural pattern closely aligned with standard LDH references, confirming high phase purity, strong interlayer periodicity, and optimal synthesis conditions for high-quality crystalline formation.

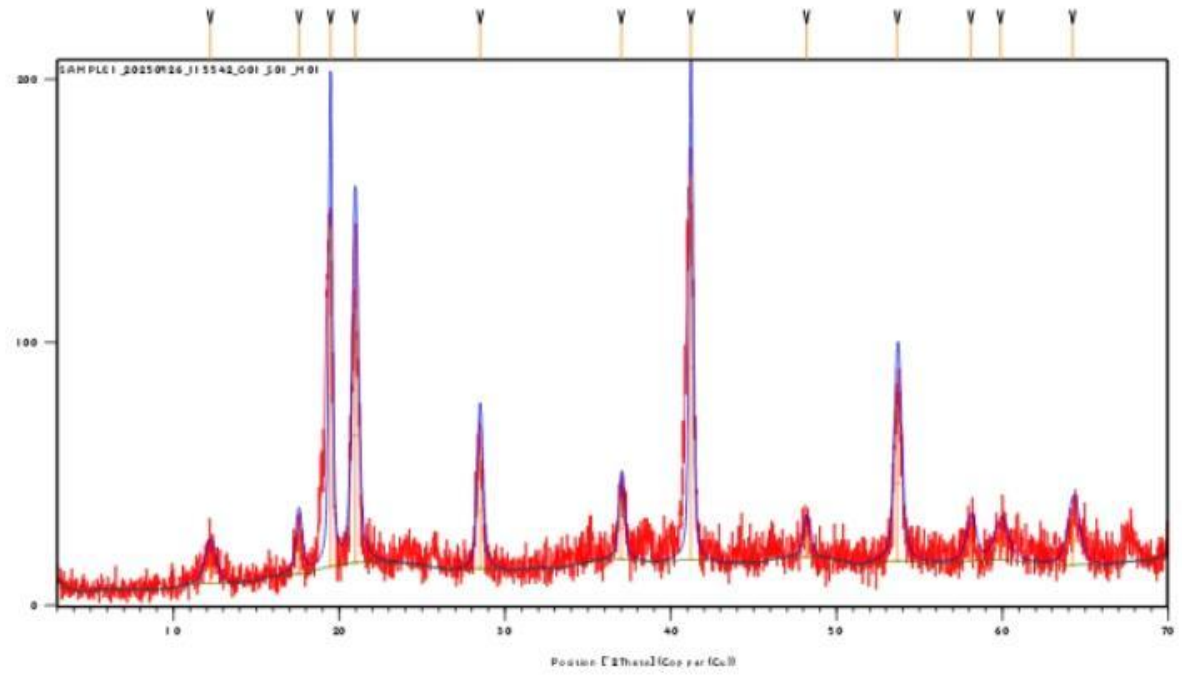

Figure 3.1: X-ray Diffraction (XRD) Pattern of Modified Zn–Al LDH (Sample 1)
Sharp peaks between 20°–60° (2θ) confirm high crystallinity and structural integrity.

Unmodified Zn–Al LDH (Sample 2)

Diffraction Pattern and Structural Features

The unmodified Zn–Al LDH showed broad, low-intensity peaks, suggesting low crystallinity and partial amorphousness. The absence of sharp reflections indicated incomplete structural development.

2θ (°)	Intensity (counts)	FWHM (°)	d-spacing (Å)	Relative Intensity (%)
11.6227	70.37	0.5510	7.6139	100
23.2246	45.10	0.6298	3.8300	65
60.4544	17.32	0.4723	1.5313	25

The main reflection at **2θ = 11.62° (d = 7.61 Å)** represented the LDH interlayer spacing, but broad **FWHM values (0.55°–0.63°)** revealed small crystallites and poor ordering.

Crystallite Size Calculation

For 2θ = 11.62° (θ = 5.81°, β = 0.0096 radians):

D = (0.9 × 1.5406) / (0.0096 × cos 5.81°) ≈ 14.5 nm

This smaller size implies a nanocrystalline or semi-amorphous structure.

Phase Identification

Under identical database conditions, the unmodified sample showed weak phase matches due to poor peak resolution. This suggested partial amorphousness and incomplete LDH formation,

possibly caused by insufficient pH control, temperature instability, or improper drying during synthesis.

The unmodified sample displayed poor crystallinity, broad peaks, and smaller crystallite domains, signifying incomplete layer formation. This explains its reduced structural order and potential inefficiency in adsorption applications.

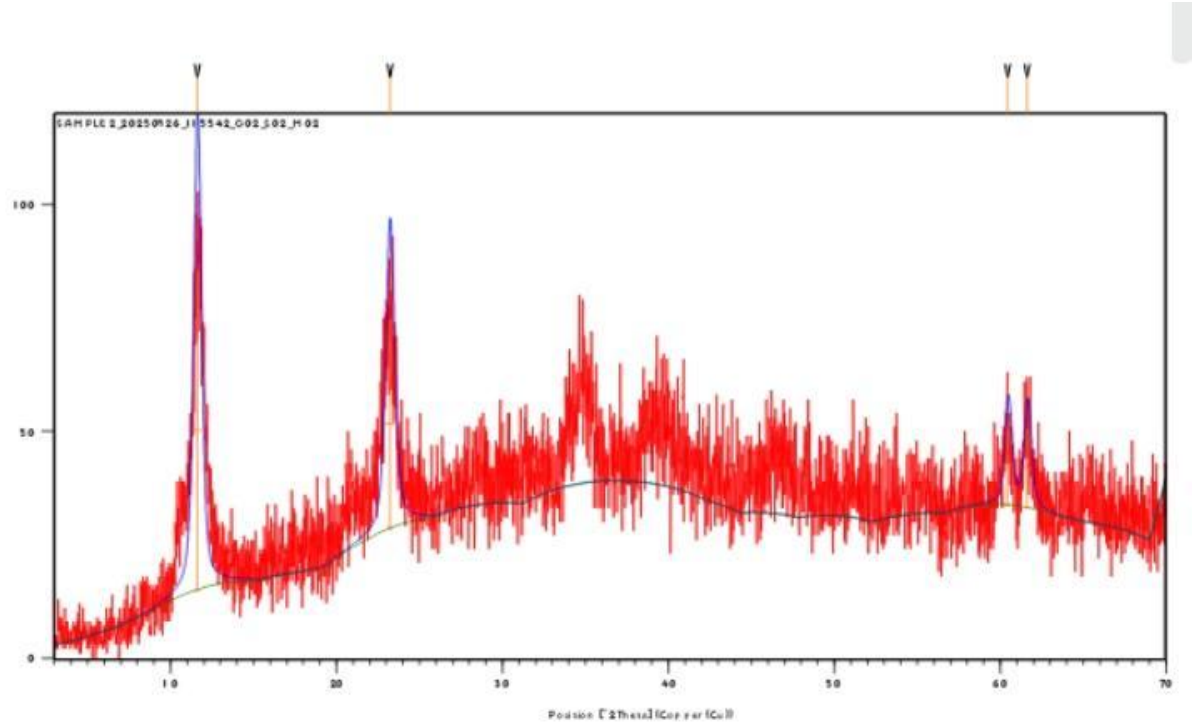

Figure 3.2: X-ray Diffraction (XRD) Pattern of Unmodified Zn–Al LDH (Sample 2) *Broad, weak peaks indicate partial amorphousness and poor crystalline quality.*

Overall Discussion

The comparison between modified and unmodified Zn–Al LDHs revealed a stark difference in structural quality. The modified sample demonstrated sharper peaks, higher crystallinity, and better structural coherence, indicating successful synthesis and phase stability. In contrast, the unmodified sample showed low crystallinity and partial amorphous characteristics, confirming that synthesis parameters (like temperature, pH, and drying) strongly affect the crystalline evolution of LDHs.

The enhanced crystallinity of the modified LDH translates to higher surface area, improved stability, and increased active adsorption sites, making it superior for environmental remediation applications such as atrazine removal. Meanwhile, the unmodified sample's poor structure limits its efficiency and stability.

In summary, XRD characterization conclusively verified that optimized synthesis produced a well-crystallized Zn–Al LDH, while inadequate conditions resulted in partial amorphousness and reduced structural integrity.

3.1.3. Powder X-Ray Diffraction (PXRD) Phase Identification of Zn–Al LDH

Purpose of PXRD Analysis

The PXRD analysis was performed to identify the crystalline phases present in the modified (Sample 1) and unmodified (Sample 2) Zn–Al LDH materials, and to determine their degree of crystallinity. PXRD provides detailed information about the atomic arrangement of materials by comparing the experimental diffraction patterns with reference data from crystallographic databases. This analysis confirmed whether the synthesis produced the expected crystalline structures, evaluated phase purity, and assessed the structural stability of each sample.

Modified Zn–Al LDH (Sample 1)

PXRD Pattern Overview

The PXRD pattern of Sample 1 showed sharp and high-intensity peaks, representing a highly crystalline material. The pattern comparison with the ICDD/JCPDS database confirmed the main phase as Bayerite ($Al(OH)_3$), with Zincite (ZnO) and Quartz (SiO_2) appearing in minor and trace quantities.

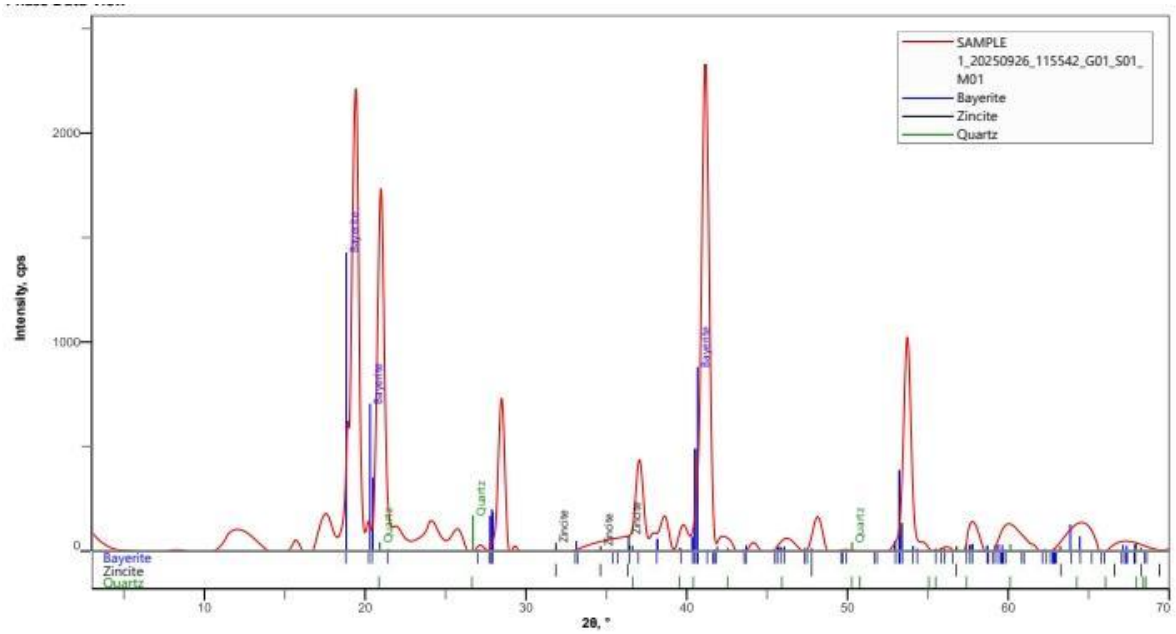

Figure 3.3: PXRD Pattern of Modified Sample 1

Sharp, high-intensity peaks confirm high crystallinity with Bayerite as the dominant phase.

Identified Crystalline Phases

The modified LDH sample exhibited three crystalline phases:

- **Major phase:** Bayerite ($Al(OH)_3$), confirming a highly ordered aluminum hydroxide structure.
- **Minor phase:** Zincite (ZnO), likely from localized zinc-rich regions during synthesis.
- **Trace phase:** Quartz (SiO_2), possibly from minimal contamination, with no major structural effect.

Peak Broadening and Crystallite Size

The sharp and narrow peaks of Sample 1 indicated large crystallite domains. Using the Scherrer equation ($D = K\lambda / \beta\cos\theta$), with ($K = 0.9$) and ($\lambda = 1.5406$ Å), the average crystallite size was calculated to be 38–40 nm. This shows that the modified sample had excellent structural order and crystal growth.

The PXRD results confirm that the modified Zn–Al LDH (Sample 1) is highly crystalline, dominated by Bayerite with minor Zincite and Quartz phases. The modification improved crystal uniformity and enhanced structural stability, producing a well-organized layered material suitable for adsorption and catalytic applications.

Unmodified Zn–Al LDH (Sample 2)

PXRD Pattern Overview

The unmodified sample exhibited broad and weak diffraction peaks, signifying poor crystallinity and partial amorphousness. The patterns showed overlapping reflections, indicating a mixture of disordered phases.

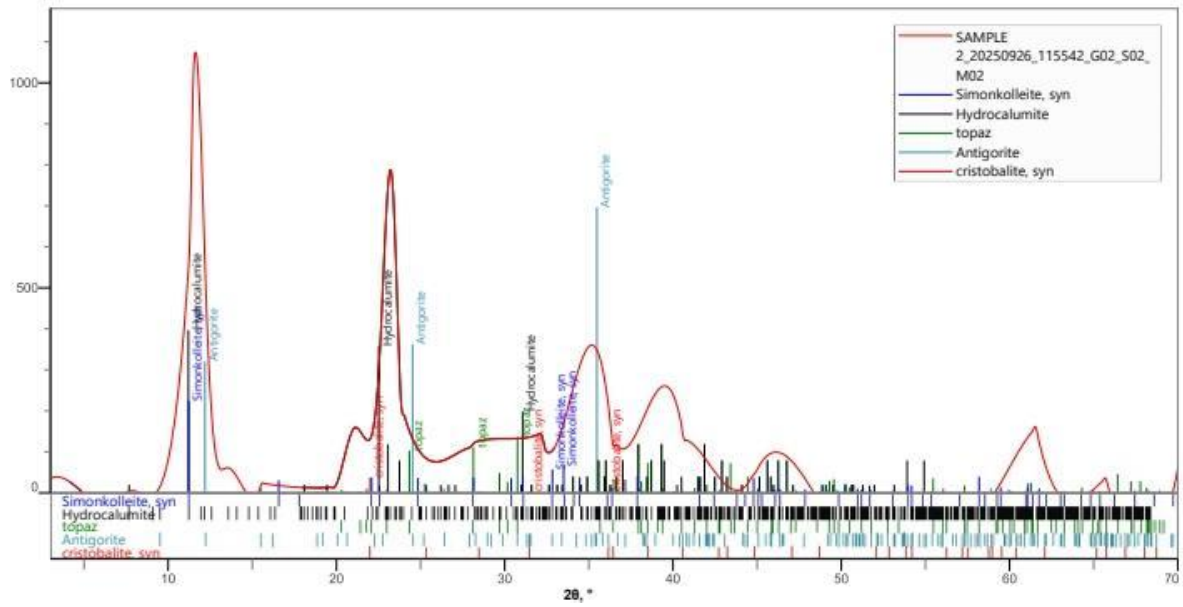

Figure 3.4: PXRD Pattern of Unmodified Sample 2

Broad, low-intensity peaks reveal poor crystallinity and multiphase structure.

Phase Identification Results

The PXRD pattern of Sample 2 showed partial alignment with several reference phases, including Simonkolleite, Hydrocalumite, Antigorite, Topaz, and Cristobalite. However, since no calcium precursor was used, Hydrocalumite's appearance was likely due to structural similarity rather than actual presence. These results confirm a disordered LDH structure mainly composed of zinc and aluminum layers, consistent with Zn–Al LDH systems.

Peak Broadening and Crystallite Size

Broad peaks indicated smaller crystallites and limited atomic ordering. Using the Scherrer equation, the average crystallite size was estimated at 14–15 nm, confirming the nanocrystalline and partially amorphous nature of the unmodified material.

The PXRD data revealed that Sample 2 is a nanocrystalline multiphase LDH with high structural disorder and low crystallinity. Its overlapping peaks and chemical heterogeneity suggest incomplete structural formation during synthesis, resulting in a less stable and less ordered framework.

Comparative Structural Behavior

Feature	**Sample 1 (Modified)**	**Sample 2 (Unmodified)**
Synthesis Outcome	Highly ordered, crystalline Al/Zn composite	Disordered, multiphase Al/Zn/Si/Mg composite
PXRD Phase Identity	Bayerite ($Al(OH)_3$), Zincite (ZnO), Quartz (SiO_2)	Simonkolleite, Hydrocalumite, Antigorite, Topaz, Cristobalite
Structural State	Large crystallites (~38–40 nm), sharp peaks	Small crystallites (~14–15 nm), broad peaks
Crystallinity	High; well-ordered structure	Low; partially amorphous and disordered
Phase Purity	Major single phase with minor traces	Multiphasic; no dominant single phase

In conclusion, the PXRD analysis clearly differentiates the structural behavior of both samples. The modified Zn–Al LDH (Sample 1) showed high crystallinity, phase purity, and structural uniformity, confirming the success of modification in producing a stable, well-ordered material. In contrast, the unmodified sample (Sample 2) exhibited poor crystallinity, multiphase composition, and partial amorphousness, indicating incomplete structural development.

Thus, the modification process significantly improved the crystal structure, phase integrity, and overall quality of the Zn–Al LDH.

3.1.4. Quantitative X-Ray Diffraction (QXRD) Analysis

Purpose of the Analysis

The Quantitative X-Ray Diffraction (QXRD) analysis was carried out to determine the weight percentages of crystalline phases present in Sample 1 after synthesis. The Rietveld refinement method was used to match experimental diffraction patterns with theoretical models of known crystalline phases. This approach provided accurate phase proportions, confirming the material's crystallinity and structural integrity. The high precision of the refinement validates the synthesis process and confirms the material's suitability for adsorption, catalysis, and other surface-based applications.

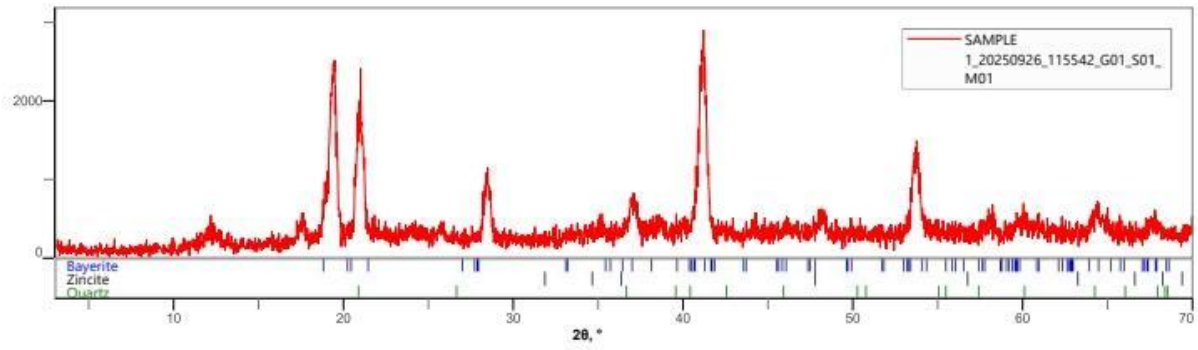

Figure 3.5: Quantitative X-ray diffraction (QXRD) pattern of Sample 1 showing the Rietveld refinement fit between experimental (red) and calculated (black) data, with the difference plot (blue).

The close alignment between both patterns and minimal residual differences indicate excellent refinement accuracy. The sharp peaks confirm multiple crystalline phases, each representing distinct atomic arrangements.

Crystalline Phase Composition (Sample 1)

Crystalline Phase	Chemical Formula	Weight Fraction (wt%)	Uncertainty (±%)	Structural Role
Bayerite	$Al(OH)_3$	69.0	±4.0	Primary aluminum-based crystalline phase
Zincite	ZnO	27.0	±4.0	Secondary zinc-based crystalline phase
Quartz	SiO_2	4.6	±6.0	Trace impurity phase

The data show that the material primarily contains Bayerite (69 wt%) and Zincite (27 wt%), with a minor Quartz impurity (4.6 wt%). This confirms successful synthesis of an aluminum–zinc hybrid crystalline material.

Structural Interpretation

a) High Crystallinity:

Sharp and well-defined peaks indicate an ordered crystalline structure dominated by Bayerite and Zincite.

b) Composite Nature:

The Bayerite–Zincite ratio (2:1) confirms a dual-phase aluminum–zinc composite structure. This configuration enhances surface reactivity and thermal stability, suitable for catalytic and adsorption applications.

c) Impurity Influence:

The small Quartz fraction likely originated from trace impurities but has no significant effect on material behaviour.

In summary, Sample 1 is a highly crystalline aluminum–zinc composite containing Bayerite (69 ± 4 wt%), Zincite (27 ± 4 wt%), and minor Quartz (4.6 ± 6 wt%). The dual-phase structure ensures good crystallinity, thermal stability, and suitability for surface-based applications.

Quantitative X-Ray Diffraction (QXRD) Analysis of Sample 2

The QXRD analysis of Sample 2 quantified its crystalline phases. Unlike Sample 1, Sample 2 exhibited a chemically complex, disordered, multiphase structure. The Rietveld refinement was used to resolve overlapping peaks and quantify phase proportions with statistical accuracy. The analysis was correlated with X-Ray Fluorescence (XRF) data to provide a complete structural understanding.

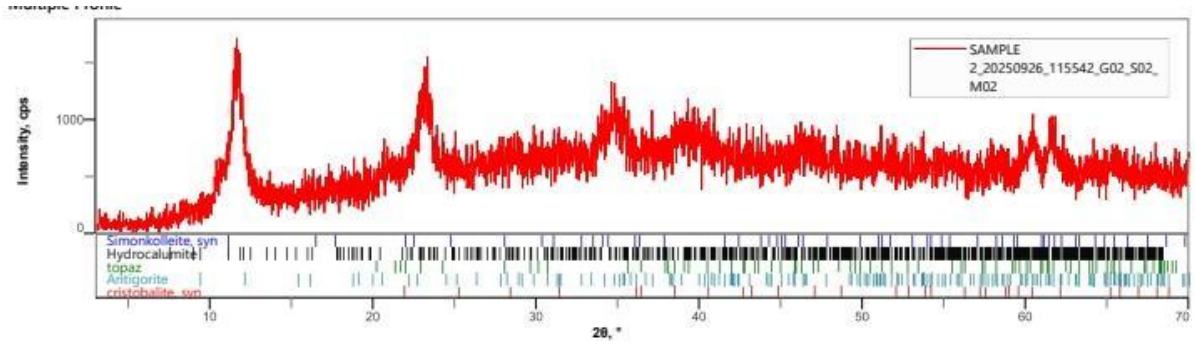

Figure 3.6: Quantitative X-ray diffraction (QXRD) pattern of Sample 2 showing overlapping peaks characteristic of a multi-phase, nanocrystalline system.

Crystalline Phase Composition (Sample 2)

Crystalline Phase	Weight Fraction (wt%)	Uncertainty (±%)	Chemical / Structural Role
Simonkolleite (synthetic)	48.0	±3.0	Dominant zinc chlorohydroxide phase [$Zn_5(OH)_8Cl_2 \cdot H_2O$]
Hydrocalumite	18.2	±17.0	Secondary Ca–Al layered double hydroxide
Topaz	16.0	±3.0	Aluminum silicate fluoride ($Al_2SiO_4F_2$) phase
Antigorite	9.6	±4.0	Mg–Fe silicate impurity
Cristobalite (synthetic)	8.0	±6.0	Silica polymorph (SiO_2); minor phase

Simonkolleite is the dominant phase (48 wt%), with significant Hydrocalumite and Topaz, and minor Antigorite and Cristobalite impurities.

Structural Interpretation

a) Structural Disorder:

High uncertainties, especially for Hydrocalumite (±17%), indicate poor long-range order and overlapping peaks typical of nanocrystalline systems.

b) Multi-Phase Nature:

The presence of five crystalline models suggests a chemically mixed composite rather than a

single compound. Rapid co-precipitation or low-temperature synthesis likely caused this structural heterogeneity.

Correlation Between XRD and XRF Results

Component Group	XRF Chemical Confirmation	XRD Structural Confirmation
Zinc–Chloride Core	High ZnO (37.04%) and Cl (1.44%) contents	Formation of Simonkolleite (48%) confirming Zn–Cl phase
Silicate Network	High SiO_2 (16.34%) content	Presence of Topaz (16%) and Cristobalite (8%) validating silicate phases
Aluminum Fraction	Low Al_2O_3 (0.24%) content	Weak Hydrocalumite (18.2%) with high uncertainty

Discussion

The coexistence of multiple crystalline phases and broad peaks confirms that Sample 2 is a nanocrystalline, structurally disordered material. Overlapping peaks indicate short-range atomic order and mixed bonding (metal–oxygen, hydroxide, and chloride). The dominant Simonkolleite phase reflects efficient zinc–chloride formation, while secondary silicate and hydroxide phases arise from concurrent side reactions involving silicon, aluminum, and magnesium impurities.

3.1.5. Fourier Transform Infrared (FTIR) Spectroscopy Analysis

FTIR Spectroscopy Analysis of Sample 1

Purpose of the Analysis

Fourier Transform Infrared (FTIR) spectroscopy was used to identify the functional groups and bonding environments in the synthesized Sample 1. The spectrum was recorded in transmittance mode within 4000–650 cm^{-1}, and the obtained peaks were matched with standard literature for metal hydroxides, oxides, and residual organics.

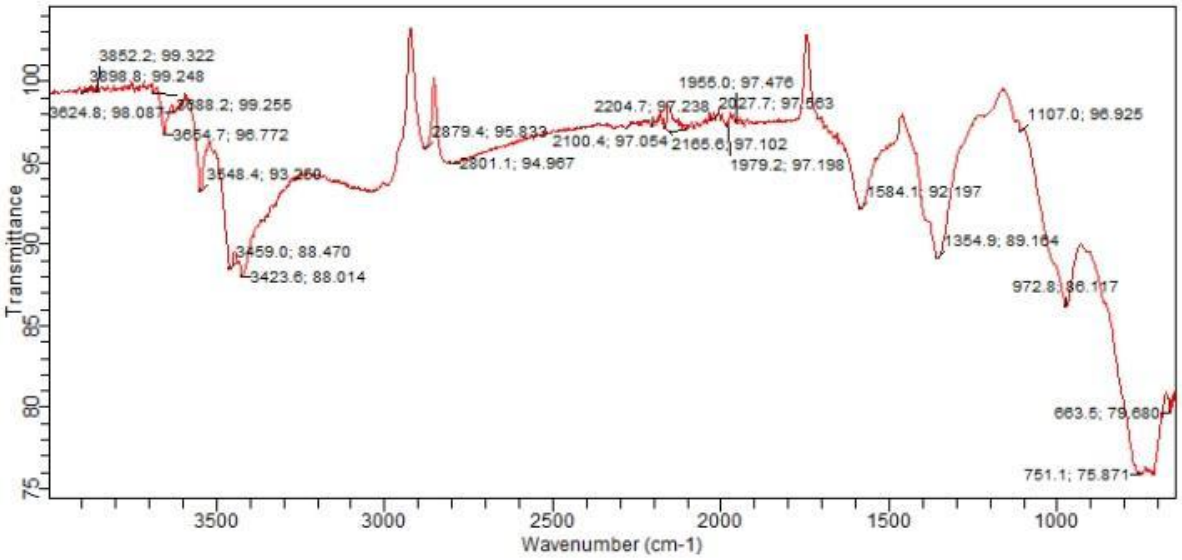

Figure 3.7: FTIR spectrum of Modified LDH showing O–H, C–H, carboxylate, and M–O vibrations confirming the inorganic Al–Zn hydroxide composition.

FTIR Peak Assignments and Interpretations for Sample 1

Wavenumber (cm^{-1})	**Assignment / Bond**	**Intensity**	**Interpretation**
3624–3400	ν(O–H) broad stretch	Medium–strong	Indicates structural hydroxyls and adsorbed water, confirming the presence of bound –OH groups typical of metal hydroxides and LDH structures.
2928 & 2879	ν(C–H) aliphatic stretch	Medium–weak	Represents C–H vibrations from residual organics, suggesting trace precursor molecules or incomplete calcination.
≈1560–1350	ν(C=O) / ν(C–O) (carboxylate modes)	Medium–weak	Shows carboxylate or carbonate groups, confirming partial organic–metal coordination.
1107–972	ν(M–O–C) / ν(M–O–M)	Medium–weak	Reflects metal–oxygen framework formation and transition from organic to inorganic bonding.
751 & 663	ν(M–O) lattice vibrations	Strong	Characteristic of Zn–O and Al–O modes, confirming Bayerite ($Al(OH)_3$) and Zincite (ZnO) phases observed in XRD.

Interpretation for Sample 1: The FTIR spectrum reveals both organic and inorganic features. The broad O–H band (3624–3400 cm^{-1}) confirms hydroxyl groups and adsorbed moisture, typical of aluminum hydroxide-based materials. The weak C–H (2928, 2879 cm^{-1}) and carboxylate (1560–1350 cm^{-1}) bands indicate minor organic residues. The fingerprint

region (1107–972 cm^{-1}) shows metal–oxygen network development, while strong M–O peaks (751 and 663 cm^{-1}) confirm Al–O and Zn–O lattice formation. When correlated with XRD and TGA results, these findings confirm a stable, ordered Al–Zn hydroxide composite with minimal organic content. The organic absorptions align with intermediate weight loss in TGA, indicating decomposition of residual organics and surface water.

In summary, Sample 1 (4000–650 cm^{-1}) is a crystalline Al–Zn hydroxide composite containing structural hydroxyls, metal–oxygen bonds, and trace organics. Strong M–O peaks verify Bayerite and Zincite formation, while weak organic signals reflect minor synthesis residues.

FTIR Spectroscopy Analysis of Sample 2

The FTIR spectrum of Sample 2 was recorded within the same wavenumber range (4000–650 cm^{-1}). The spectral profile showed fewer and broader peaks, indicating a nanocrystalline or partially amorphous structure.

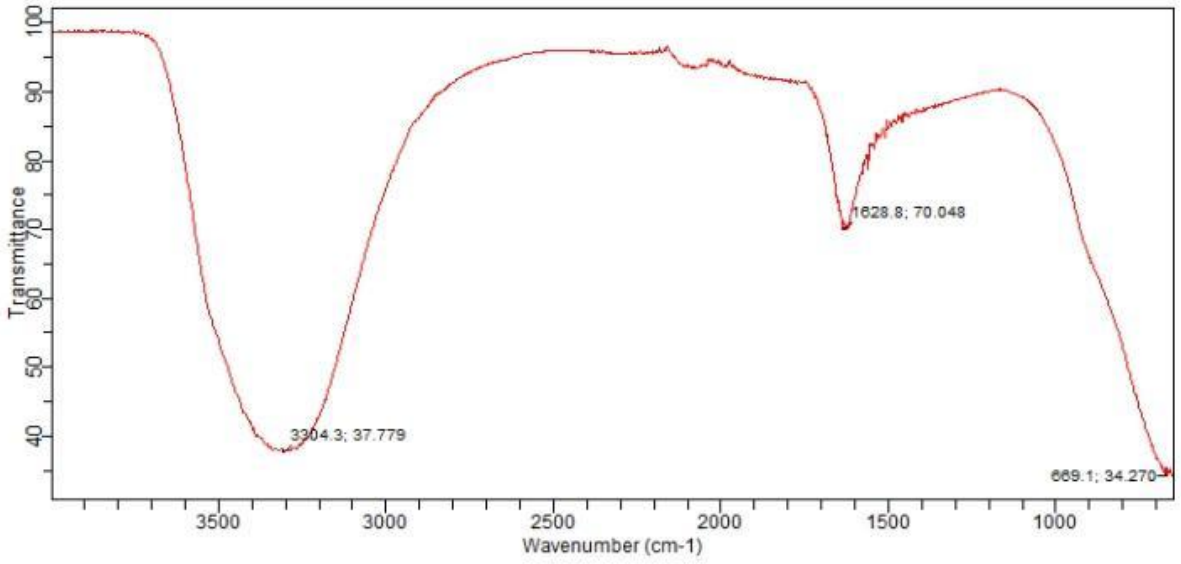

Figure 3.8: FTIR spectrum of Unmodified LDH showing broad O–H and M–O absorptions (4000–650 cm^{-1}).

FTIR Peak Assignments and Interpretations for Sample 2

Wavenumber (cm^{-1})	Functional Group / Bond	Intensity and Shape	Interpretation
3304.3	ν(O–H) stretching	Extremely broad	Represents numerous hydroxyls from structural and surface water; extensive hydrogen bonding typical of nanocrystalline materials.
1628.8	δ(H–O–H) bending	Medium–strong	Confirms molecular water presence and interlayer moisture.
669.1	ν(M–O) lattice vibration	Broad, low resolution	Indicates metal–oxygen stretching; the diffuse nature reflects structural disorder and short-range order.

Interpretation for Sample 2

The spectrum displays broad O–H and H–O–H bands, confirming a hydroxyl-rich, moisture-absorbing surface. The absence of C–H and carboxylate bands shows complete organic decomposition. The broad M–O peak (669 cm^{-1}) reflects a disrupted metal–oxygen network lacking long-range order, consistent with XRD results showing broad peaks and 14.5 nm crystallite size.

In summary, Sample 2 is a nanocrystalline inorganic oxide with high hydroxyl content and structural disorder. The broad O–H (3304 cm^{-1}) and M–O (669 cm^{-1}) bands confirm short-range atomic order, high defect density, and total removal of organic residue

Comparative Discussion of FTIR and XRD

Feature	Sample 1 – Highly Crystalline Product	Sample 2 – Nanocrystalline Product
XRD Pattern	Sharp, intense diffraction peaks	Broad, low-intensity peaks
XRD Interpretation	Highly crystalline with large domains	Nanocrystalline with high disorder (~14.5 nm)
Thermal Decomposition	Sharp mass loss (~375 °C)	Gradual, extended mass loss (>375 °C)
FTIR Metal–Oxygen Peaks	Sharp (751, 663 cm^{-1})	Broad band (~669 cm^{-1})
FTIR O–H / Water Features	Moderate, well-defined	Intense, extremely broad (3304, 1628 cm^{-1})
Organic Residues	Present (C–H, COO^- bands)	Absent (no organic vibrations)
Overall Conclusion	Crystalline Al–Zn oxide with residual organics	Nanocrystalline Zn–Si oxide with high hydroxylation and disorder

Discussion

The comparative FTIR and XRD data confirm major structural differences between both samples. Sample 1 exhibits a well-ordered Al–Zn hydroxide framework, while Sample 2 shows a disordered nanocrystalline oxide. Variations in synthesis conditions such as temperature and aging produced these distinct outcomes.

The disappearance of organic bands and broadening of O–H and M–O regions in Sample 2 indicate complete decomposition of organics and increased structural defects. These results confirm that small synthesis changes significantly affect crystallinity, surface chemistry, and material performance.

3.2 **Effect Of Weight On Contact Time**

The equation of a straight line graph

$R^2 = 0.9905$

$Y = 0.2076x + 0.3733$

Y= Absorbance (A)

X= equilibrium concentration

therefore

$A = 0.2076x + 0.3733$

$X = A - 0.3733 / 0.2076$

Terms definition:

- Time - contact time(mins)
- Weight – mass of LDH (g)
- Concentration – concentration of atrazine solution
- Absorbance – Absorbance values gotten from the uv–vis spectrometer
- Ce – initial concentration of atrazine
- Ct – concentration of atrazine at time t
- Co - ct – amount adsorbed i e the amount of atrazine that has been removed from the solution
- qt – Absorption capacity i.e amount of atrazine was adsorbed per gram of adsorbent
- % adsorbed – percentage of atrazine that was removed from solution

Table 3.2.1. Effect of 0.1g of EDTA Modified LDH on 100mg/L of Atrazine

Time (min)	Weight (g)	Co (mg/L)	Absorbance (A)	Ct (mg/L) = A– 0.3733/0.2076	Amount Adsorbed (mg/L) (Co – Ce)	q_t (Co – Ce) * V / weight	% Adsorbed (Co – Ce) x 100/Co
1	0.1	100	2.403	97.582	2.418	2.418	2.42%
2	0.1	100	2.355	95.274	4.726	4.726	4.73%
5	0.1	100	2.323	93.736	6.264	6.264	6.26%
10	0.1	100	2.190	87.341	12.659	12.659	12.66%
15	0.1	100	2.140	84.938	15.063	15.063	15.06%
30	0.1	100	1.881	72.486	27.514	27.514	27.51%
45	0.1	100	1.653	61.524	38.476	38.476	38.48%
60	0.1	100	1.540	56.091	43.909	43.909	43.91%
90	0.1	100	1.395	49.120	50.880	50.880	50.88%
120	0.1	100	1.280	43.591	56.409	56.409	56.41%
180	0.1	100	1.164	38.014	61.986	61.986	61.99%
240	0.1	100	1.058	32.918	67.082	67.082	67.08%
300	0.1	100	1.008	30.514	69.486	69.486	69.49%

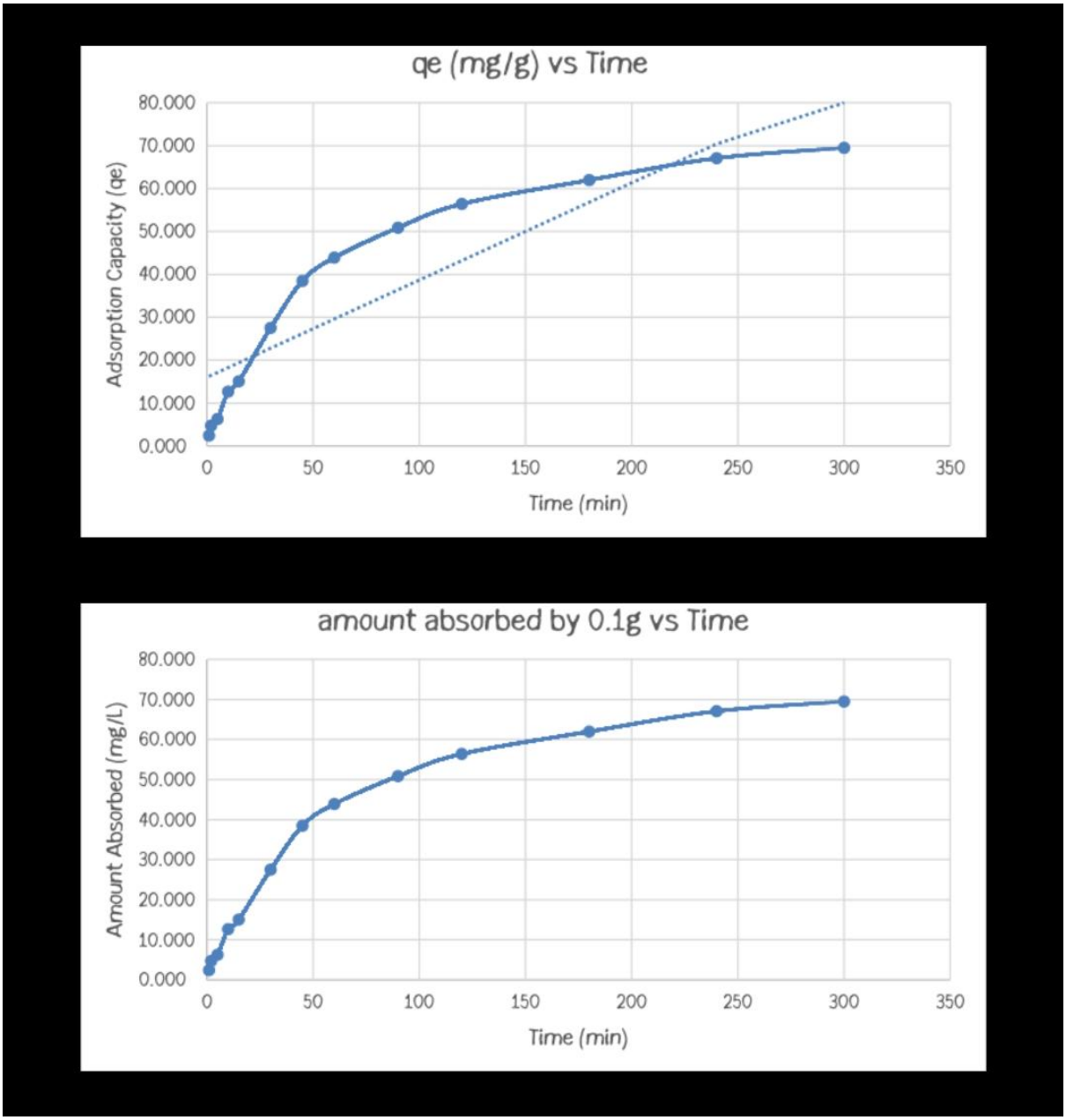
qe (mg/g) vs Time
Adsorption Capacity (qe)
80.000
70.000
60.000
50.000
40.000
30.000
20.000
10.000
0.000
0
50
100
150
200
250
300
350
Time (min)
amount absorbed by 0.1g vs Time
Amount Absorbed (mg/L)
80.000
70.000
60.000
50.000
40.000
30.000
20.000
10.000
0.000
0
50
100
150
200
250
300
350
Time (min)

Table 3.2.2. Effect of 0.3g of EDTA Modified LDH on 100mg/L of Atrazine

Time (min)	Weight (g)	Co (mg/L)	Absorbance (A)	Ct (mg/L) A– 0.3733/0.2076	Amount Adsorbed (mg/L) (Co – Ce)	Co – Ce) * V / weight qt	% Adsorbed
1	0.3	100	2.317	93.447	6.553	2.184	6.55%
2	0.3	100	2.231	89.313	10.688	3.563	10.69%
5	0.3	100	2.070	81.572	18.428	6.143	18.43%
10	0.3	100	2.004	78.399	21.601	7.200	21.60%
15	0.3	100	1.811	69.120	30.880	10.293	30.88%
30	0.3	100	1.525	55.370	44.630	14.877	44.63%
45	0.3	100	1.210	40.226	59.774	19.925	59.77%
60	0.3	100	1.192	39.361	60.639	20.213	60.64%
90	0.3	100	1.063	33.159	66.841	22.280	66.84%
120	0.3	100	1.045	32.293	67.707	22.569	67.71%
180	0.3	100	0.941	27.293	72.707	24.236	72.71%
240	0.3	100	0.927	26.620	73.380	24.460	73.38%
300	0.3	100	0.953	27.870	72.130	24.043	72.13%

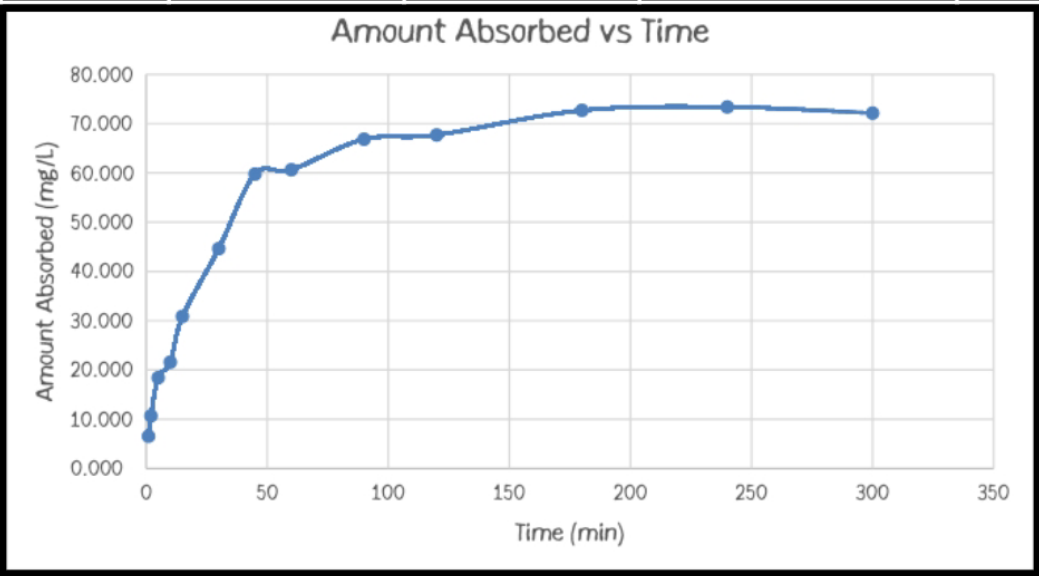
Amount Absorbed vs Time
Amount Absorbed (mg/L)
80.000
70.000
60.000
50.000
40.000
30.000
20.000
10.000
0.000
0
50
100
150
200
250
300
350
Time (min)

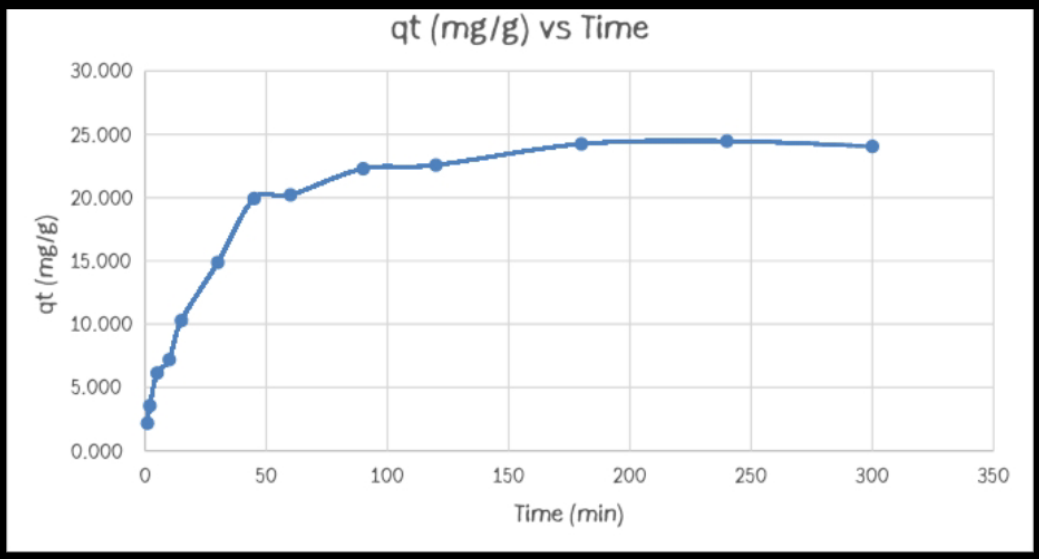
qt (mg/g) vs Time
qt (mg/g)
30.000
25.000
20.000
15.000
10.000
5.000
0.000
0
50
100
150
200
250
300
350
Time (min)

Table 3.2.3 Effect of 0.5g of EDTA Modified LDH on 100mg/L of Atrazine

Time (min)	Weight (g)	Co (mg/L)	Absorbance (A)	Ct (mg/L)	Amount Adsorbed (mg/L) (Co – Ce)	(Co – Ce) * V / weight qt	% Adsorbed
1	0.5	100	2.048	80.514	19.486	3.897	19.49%
2	0.5	100	2.007	78.543	21.457	4.291	21.46%
5	0.5	100	1.972	76.861	23.139	4.628	23.14%
10	0.5	100	1.856	71.284	28.716	5.743	28.72%
15	0.5	100	1.775	67.389	32.611	6.522	32.61%
30	0.5	100	1.597	58.832	41.168	8.234	41.17%
45	0.5	100	1.309	44.986	55.014	11.003	55.01%
60	0.5	100	1.217	40.563	59.438	11.888	59.44%
90	0.5	100	1.082	34.072	65.928	13.186	65.93%
120	0.5	100	0.995	29.889	70.111	14.022	70.11%
180	0.5	100	0.979	29.120	70.880	14.176	70.88%
240	0.5	100	0.971	28.736	71.264	14.253	71.26%
300	0.5	100	0.953	27.870	72.130	14.426	72.13%

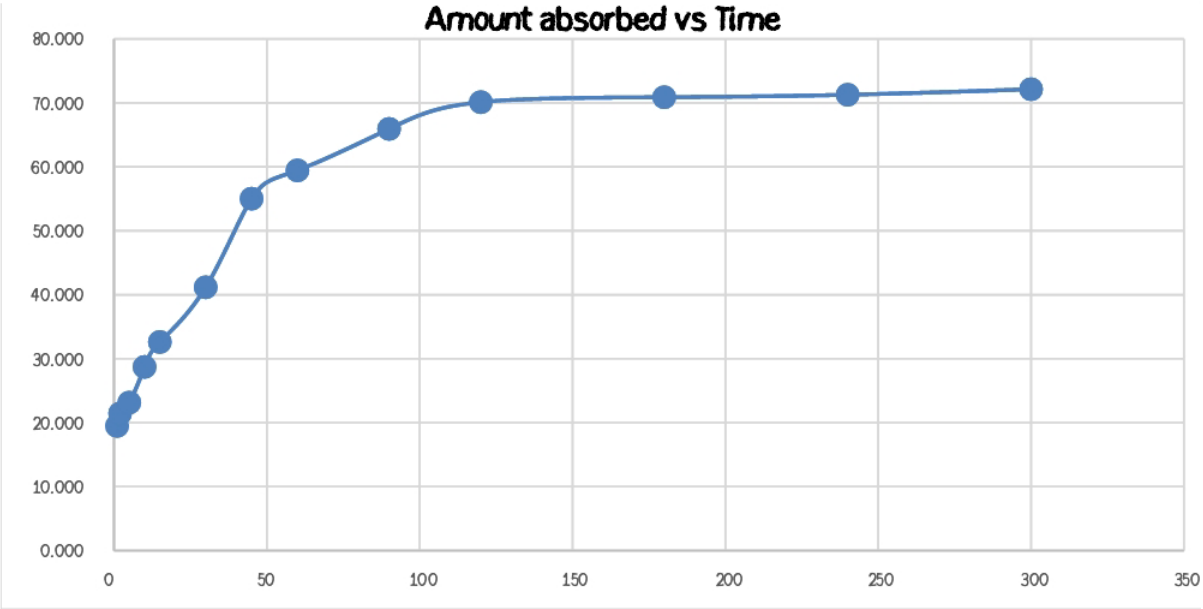
Amount absorbed vs Time
80.000
70.000
60.000
50.000
40.000
30.000
20.000
10.000
0.000
0
50
100
150
200
250
300
350

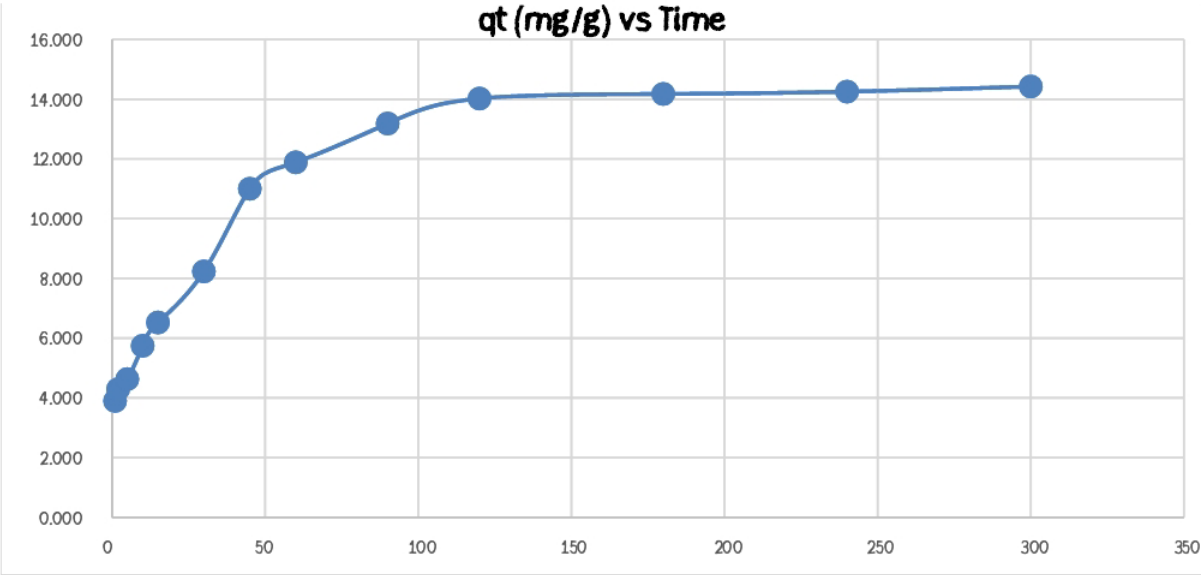
qt (mg/g) vs Time
16.000
14.000
12.000
10.000
8.000
6.000
4.000
2.000
0.000
0
50
100
150
200
250
300
350

Table 3.2.4. Effect of 0.7g of EDTA Modified LDH on 100mg/L of Atrazine

Time (min)	Weight (g)	Co (mg/L)	Absorbance (A)	Ct (mg/L) A– 0.3733/0.2076	Amount Adsorbed (mg/L) (Co – Ce)	$q_{t\ (mg/l\ /g)}$ Co – Ce) * V / weight	% Adsorbed
1	0.7	100	2.023	79.313	20.688	2.955	20.69%
2	0.7	100	1.811	69.120	30.880	4.411	30.88%
5	0.7	100	1.709	64.216	35.784	5.112	35.78%
10	0.7	100	1.638	60.803	39.197	5.600	39.20%
15	0.7	100	1.614	59.649	40.351	5.764	40.35%
30	0.7	100	1.458	52.149	47.851	6.836	47.85%
45	0.7	100	1.052	32.630	67.370	9.624	67.37%
60	0.7	100	1.109	35.370	64.630	9.233	64.63%
90	0.7	100	0.967	28.543	71.457	10.208	71.46%
120	0.7	100	0.925	26.524	73.476	10.497	73.48%
180	0.7	100	0.920	26.284	73.716	10.531	73.72%
240	0.7	100	0.899	25.274	74.726	10.675	74.73%
300	0.7	100	0.922	26.380	73.620	10.517	73.62%

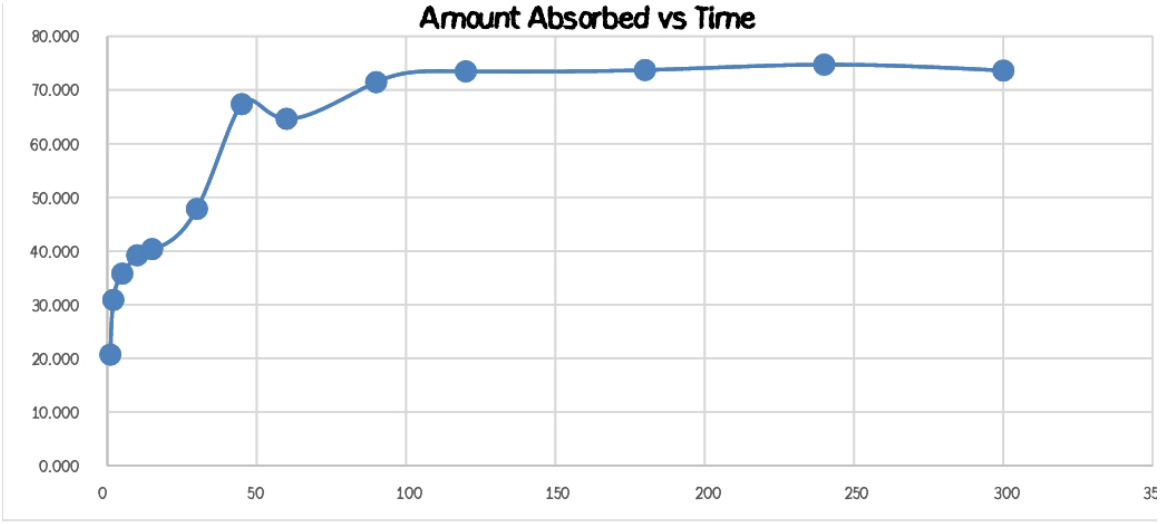
Amount Absorbed vs Time
80.000
70.000
60.000
50.000
40.000
30.000
20.000
10.000
0.000
0
50
100
150
200
250
300

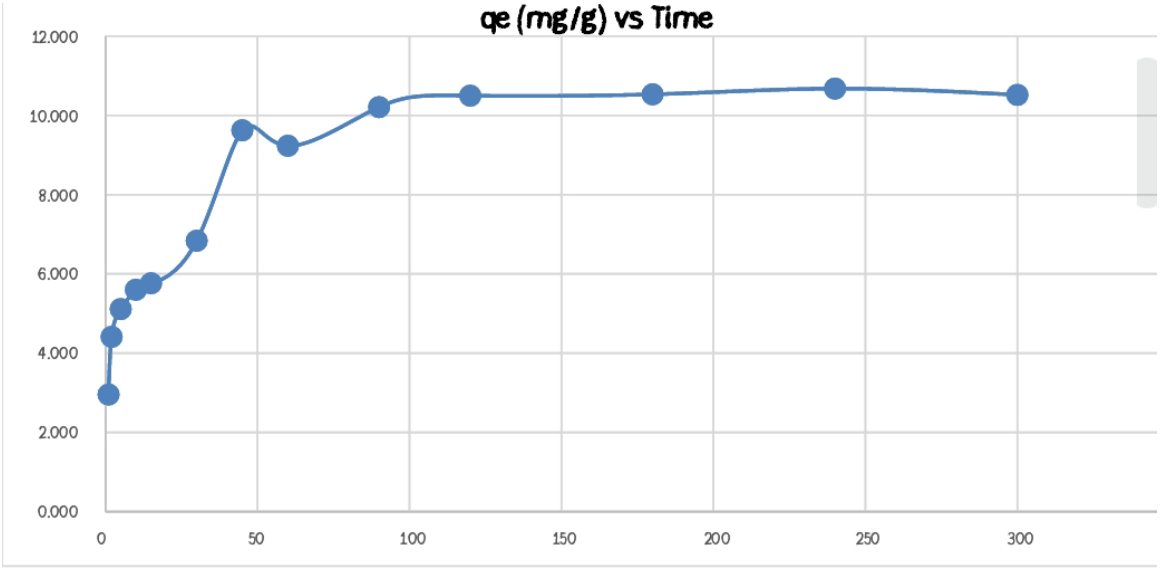
qe (mg/g) vs Time
12.000
10.000
8.000
6.000
4.000
2.000
0.000
0
50
100
150
200
250
300

Table 3.2.5. Effect of 1g of EDTA Modified LDH on 100mg/L of Atrazine

Time (min)	Weight (g)	Co (mg/L)	Absorbance (A)	Ct (mg/L) A– 0.3733/0.2076	Amount Adsorbed (mg/L) (Co – Ce)	Co – Ce) * V / weight qt (mg/l/g)	% Adsorbed
1	1.0	100	1.757	66.524	33.476	3.348	33.48%
2	1.0	100	1.547	56.428	43.572	4.357	43.57%
5	1.0	100	1.535	55.851	44.149	4.415	44.15%
10	1.0	100	1.480	53.207	46.793	4.679	46.79%
15	1.0	100	1.303	44.697	55.303	5.530	55.30%
30	1.0	100	1.076	33.784	66.216	6.622	66.22%
45	1.0	100	0.983	29.313	70.688	7.069	70.69%
60	1.0	100	0.944	27.438	72.563	7.256	72.56%
90	1.0	100	0.796	20.322	79.678	7.968	79.68%
120	1.0	100	0.789	19.986	80.014	8.001	80.01%
180	1.0	100	0.814	21.188	78.813	7.881	78.81%
240	1.0	100	0.768	18.976	81.024	8.102	81.02%
300	1.0	100	0.802	20.611	79.389	7.939	79.39%

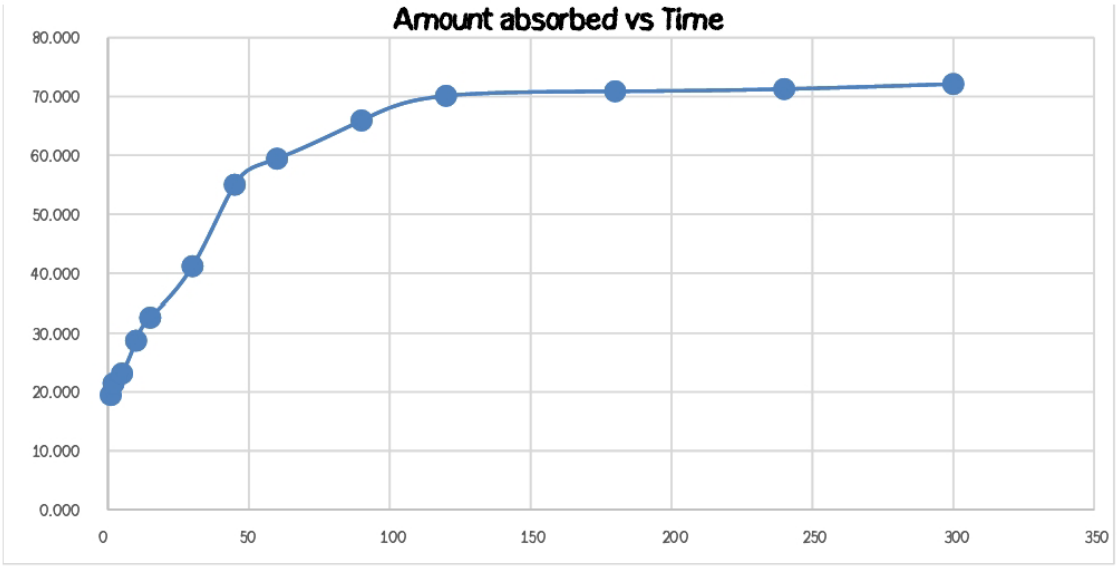
Amount absorbed vs Time
80.000
70.000
60.000
50.000
40.000
30.000
20.000
10.000
0.000
0
50
100
150
200
250
300
350

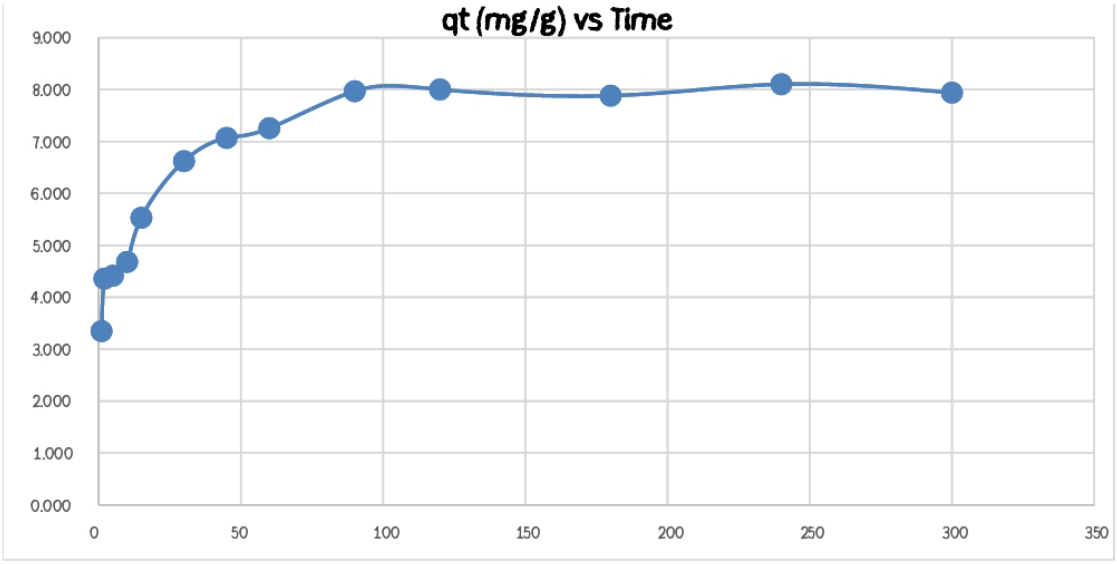
qt (mg/g) vs Time
9.000
8.000
7.000
6.000
5.000
4.000
3.000
2.000
1.000
0.000
0
50
100
150
200
250
300
350

Table 3.2.6 Effect of weight on contact time combined graph

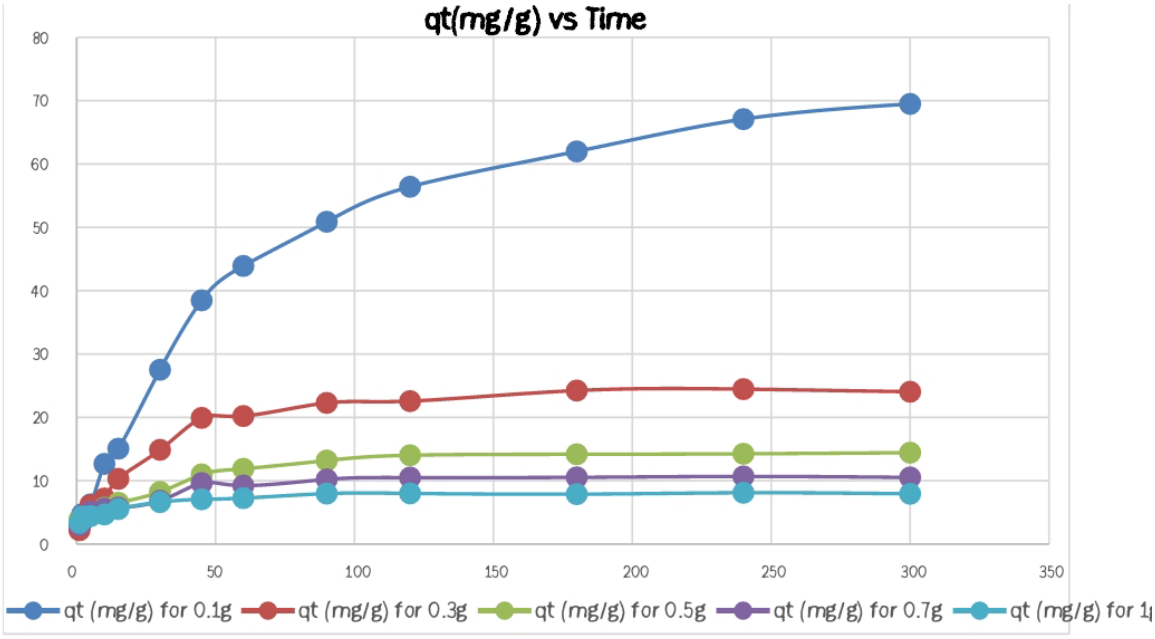

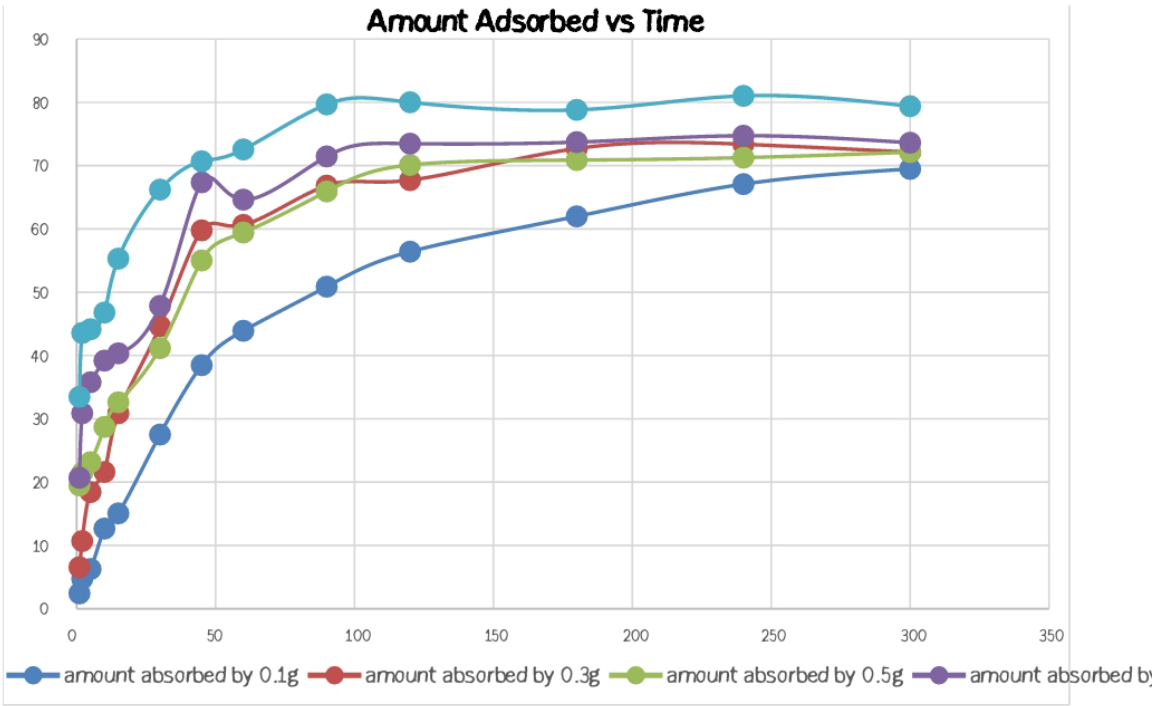

For all samples, adsorption increased rapidly during the first 30 minutes and gradually slowed as equilibrium was approached at about 300 minutes. This two-stage pattern indicates an initial surface adsorption phase followed by slower intraparticle diffusion into the LDH pores.

Increasing the adsorbent mass from 0.1 g to 1.0 g led to higher overall atrazine removal from solution but lower adsorption capacity (q_e, mg/g).

At 0.1 g, 69.5 mg/g (69%) of atrazine was removed.

At 0.3 g, removal increased to 72.1%.

At 0.5 g, about 72.1% was removed.

At 0.7 g, removal reached 74.7%.

At 1.0 g, maximum removal was observed (81%).

This shows that while more adsorbent gives greater total removal, each gram of adsorbent captures less atrazine because the available surface area per gram is underutilized.

This shows that while more adsorbent
gives greater total removal, each gram of adsorbent captures less atrazine because the available surface area per gram is underutilized.

Equilibrium was attained at approximately 240–300 minutes for all dosages, beyond which no significant increase in adsorption occurred.

The data show that adsorption of atrazine on EDTA-modified LDH is time-dependent and strongly influenced by adsorbent dose, with the process being rapid at first and slowing as surface sites become saturated.

Table 3.

Time (min)	qt	qe	qe - qt	ln(qe- qt)	t^(1/2)
1	3.348	8.102	4.754	1.558986	1
2	4.357	8.102	3.745	1.320422	1.414214
5	4.415	8.102	3.687	1.304813	2.236068
10	4.679	8.102	3.423	1.230517	3.162278
15	5.53	8.102	2.572	0.944684	3.872983
30	6.622	8.102	1.48	0.392042	5.477226
45	7.069	8.102	1.033	0.032467	6.708204
60	7.256	8.102	0.846	-0.16724	7.745967
90	7.968	8.102	0.134	-2.00992	9.486833
120	8.001	8.102	0.101	-2.29263	10.95445
180	7.881	8.102	0.221	-1.50959	13.41641
240	8.102	8.102	0	0	15.49193
300	7.939	8.102	0.163	-1.81401	17.32051

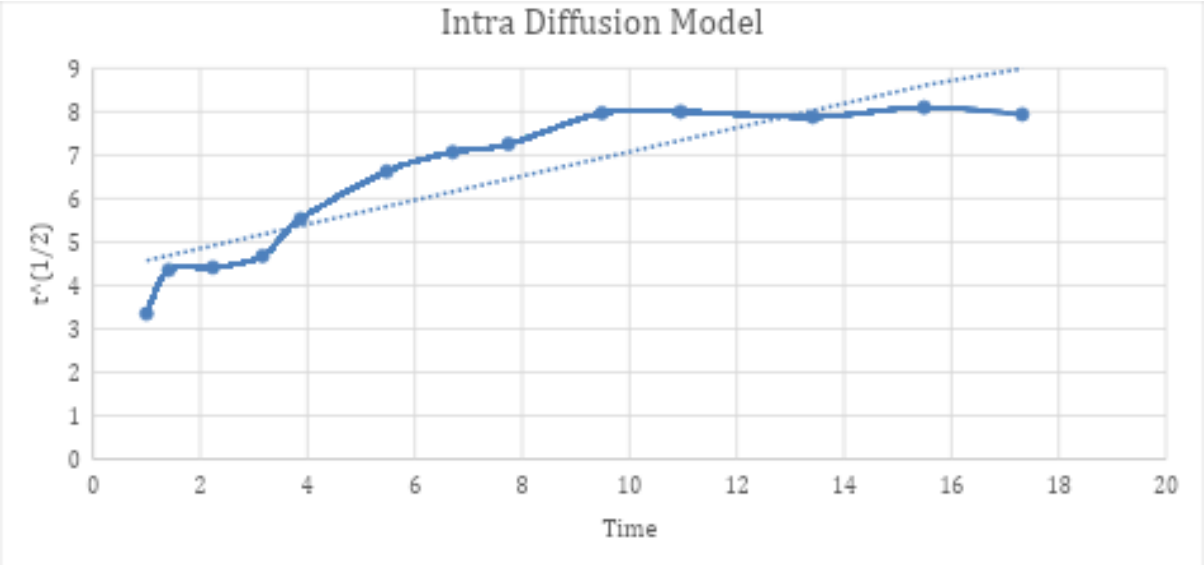

Rate constant = 0.2781

The process is diffusion-controlled (mass transfer plays a big role)

3.4. DISCUSSION

The effect of adsorbent weight on contact time was studied to understand how different dosages of EDTA-modified LDH influenced the removal of atrazine from solution over time. From the data, adsorption followed a two-phase pattern typical of solid–liquid adsorption systems. In the initial stage (0–30 minutes), the rate of adsorption increased sharply for all samples. This rapid uptake corresponds to the availability of a large number of active sites on the adsorbent surface, allowing atrazine molecules to easily attach. As time progressed, the rate gradually slowed, indicating that the readily available surface sites were becoming occupied, and further adsorption required diffusion of atrazine molecules into the interior pores of the adsorbent. This transition from a fast surface adsorption stage to a slower intraparticle diffusion stage suggests that both surface interaction and pore diffusion contributed to the overall process.

As the adsorbent weight increased from 0.1 g to 1.0 g, there was a clear improvement in the total percentage of atrazine removed from solution. Specifically, the percentage removal rose from about 69.5% for 0.1 g to approximately 81% for 1.0 g. This improvement is attributed to the increased number of available adsorption sites with higher adsorbent mass. A larger quantity of LDH means more active surfaces and binding sites for atrazine molecules, leading to greater overall removal efficiency.

However, while total removal increased, the adsorption capacity (q_e, expressed in mg of atrazine adsorbed per gram of adsorbent) decreased with increasing mass. This inverse relationship occurs because at higher adsorbent doses, the surface area per unit mass is underutilized. In other words, as more adsorbent is introduced, atrazine molecules are distributed across a larger surface area, reducing the concentration gradient and resulting in fewer atrazine molecules adsorbed per gram of LDH. This effect is known as the “adsorbent dose paradox,” where increasing the quantity of adsorbent enhances total removal but reduces adsorption efficiency per gram.

The equilibrium time for adsorption was found to be between 240 and 300 minutes for all adsorbent weights. Beyond this time, no significant increase in atrazine uptake was observed, indicating that equilibrium had been reached and all accessible binding sites were either occupied or inaccessible due to diffusion limitations. The relatively long equilibrium period implies that intraparticle diffusion plays a key role in controlling the overall rate of adsorption.

The linear relationship between absorbance (A) and equilibrium concentration (C_e), described by the equation **$A = 0.2076x + 0.3733$ ($R^2 = 0.9905$)**, confirms a strong correlation between spectrophotometric absorbance readings and the concentration of atrazine remaining in solution. The high R^2 value indicates that the equation can reliably predict concentration changes based on absorbance values, validating the UV–Vis method used for monitoring the adsorption process.

From the kinetic data, the calculated rate constant of 0.2781 suggests that the process is largely diffusion-controlled, meaning mass transfer within the pores of the adsorbent is the rate-limiting step rather than the initial surface adsorption. This supports the observation that after the rapid initial phase, the adsorption rate declined as equilibrium approached.

In summary, increasing the mass of EDTA-modified LDH enhances the overall percentage removal of atrazine but lowers the adsorption capacity per gram due to surface site overlap and particle aggregation. The adsorption process proceeds quickly at first and then slows as diffusion becomes dominant. Equilibrium is achieved within 240–300 minutes, and the high correlation between absorbance and concentration confirms the reliability of the measurements. Overall, the study demonstrates that adsorbent dosage and contact time are key parameters influencing both the kinetics and efficiency of atrazine removal by EDTA-modified LDH.

REFERENCES

Abdelkawy, A. M., Elantabli, F. M., Mahmoud, R., Mahgoub, S. M., El-Ela, F. I. A., Mohamed, H. A., & Moaty, S. A. A. (2025). Enhanced Zn-Co-Fe Layered Double Hydroxides for Effective Levofloxacin Removal: Innovation in Reuse of Waste Adsorbent. *Journal of Pharmaceutical Innovation*, *20*(3). https://doi.org/10.1007/s12247-025-09988-1

Algarni, T. saad, & Al-Mohaimeed, A. M. (2022). Water purification by absorption of pigments or pollutants via metaloxide (Review). *Journal of King Saud University - Science*, 102339. https://doi.org/10.1016/j.jksus.2022.102339

Badran, A. M., Utra, U., Yussof, N. S., & Bashir, M. J. K. (2023). Advancements in Adsorption Techniques for Sustainable Water Purification: A Focus on Lead Removal. *Separations*, *10*(11), 565. https://doi.org/10.3390/separations10110565

Das, S., Sakr, H., Al-Huseini, I., Jetti, R., Al-Qasmi, S., Sugavasi, R., & Sirasanagandla, S. R. (2023). Atrazine Toxicity: The Possible Role of Natural Products for Effective Treatment. *Plants*, *12*(12), 2278. https://doi.org/10.3390/plants12122278

De Caroli , B. V., Silva da Silva, G., Ferreira de Medeiros, J., & Montagner, C. C. (2023). Atrazine and its degradation products in drinking water source and supply: Risk assessment for environmental and human health in Campinas, Brazil. *Chemosphere*, *336*(2), 139289. https://doi.org/10.1016/j.chemosphere.2023.139289

Dehghani, M. H., Ahmadi, S., Ghosh, S., Othmani, A., Osagie, C., Meskini, M., AlKafaas, S. S., Malloum, A., Khanday, W. A., Jacob, A. O., Gökkuş, Ö., Oroke, A., Martins Chineme, O., Karri, R. R., & Lima, E. C. (2023). Recent advances on sustainable adsorbents for the remediation of noxious pollutants from water and wastewater: A critical review. *Arabian Journal of Chemistry*, *16*(12), 105303. https://doi.org/10.1016/j.arabjc.2023.105303

do Nascimento, C. T., Vieira, M. G. A., Scheufele, F. B., Palú, F., da Silva, E. A., & Borba, C. E. (2022). Adsorption of atrazine from aqueous systems on chemically activated biochar produced from corn straw. *Journal of Environmental Chemical Engineering*, *10*(1), 107039. https://doi.org/10.1016/j.jece.2021.107039

Eid Al-Rawajfeh, A., Ibrahim Alrawashdeh, A., Etiwi, M. T., Mainali, B., Shahid, M. K., Al-Itawi, H., Ehab Al-Shamaileh, Al-E'bayat, M., & Al-Sahary, A. (2025). Fabrication of Silver-Incorporated Zn-Al Layered Double Hydroxide: Characterization and Bromide-Adsorption Performance. *Water*, *17*(11), 1578–1578. https://doi.org/10.3390/w17111

Ghanbari, N., & Ghafuri, H. (2023). Preparation of novel Zn–Al layered double hydroxide composite as adsorbent for removal of organophosphorus insecticides from water. *Scientific Reports*, *13*(1). https://doi.org/10.1038/s41598-023-37070-8

Ghazi, R. M., Nik Yusoff, N. R., Halim, A., Wahab, A., Ab Latif, N., Hasmoni, S. H., Zaini, A., & Zainul Akmar Zakaria. (2023). Health effects of herbicides and its current removal strategies. *Bioengineered*, *14*(1). https://doi.org/10.1080/21655979.2023.2259526

Gkika, D. A., Tolkou, A. K., Katsoyiannis, I. A., & Kyzas, G. Z. (2025). The adsorption-desorption-regeneration pathway to a circular economy: The role of waste-derived adsorbents on chromium removal. *Separation and Purification Technology*, *368*, 132996. https://doi.org/10.1016/j.seppur.2025.132996

Hong, J., Boussetta, N., Enderlin, G., Merlier, F., & Grimi, N. (2022). Degradation of Residual Herbicide Atrazine in Agri-Food and Washing Water. *Foods*, *11*(16), 2416. https://doi.org/10.3390/foods11162416

Kameliya, J., Verma, A., Dutta, P., Arora, C., Vyas, S., & Varma, R. S. (2023). Layered Double Hydroxide Materials: A Review on Their Preparation, Characterization, and Applications. *Inorganics (Basel)*, *11*(3), 121–121. https://doi.org/10.3390/inorganics11030121

Kaur, H., Devi, N., Siwal, S. S., Alsanie, W. F., Thakur, M. K., & Thakur, V. K. (2023). Metal–Organic Framework-Based Materials for Wastewater Treatment: Superior Adsorbent Materials for the Removal of Hazardous Pollutants. *ACS Omega*, *8*(10), 9004–9030. https://doi.org/10.1021/acsomega.2c07719

Kumari, P., & Kumar, A. (2023). ADVANCED OXIDATION PROCESS: A remediation technique for organic and non-biodegradable pollutant. *Results in Surfaces and Interfaces*, *11*, 100122. https://doi.org/10.1016/j.rsurfi.2023.100122

Lartey-Young, G., & Ma, L. (2022). Optimization, equilibrium, adsorption behaviour of Cu/Zn/Fe LDH and LDHBC composites towards atrazine reclamation in an aqueous environment. *Chemosphere*, *293*, 133526–133526. https://doi.org/10.1016/j.chemosphere.2022.133526

Li, L., Soyhan, I., Warszawik, E., & van Rijn, P. (2024). Layered Double Hydroxides: Recent Progress and Promising Perspectives Toward Biomedical Applications. *Advanced Science*, *11*(20). https://doi.org/10.1002/advs.202306035

Mishra, R. K., Mentha, S. S., Misra, Y., & Dwivedi, N. (2023). Emerging pollutants of severe environmental concern in water and wastewater: A comprehensive review on current developments and future research. *Water-Energy Nexus*, *6*(1), 74–95. https://doi.org/10.1016/j.wen.2023.08.002

Mohamed, Komarla Kumarachari, R., Pawar, S., Neerugatti, D., Tefera Mekasha, Y., & Bandarapalle, K. (2025). Plasma catalysis for sustainable industry: lab-scale studies and pathways to upscaling. *Deleted Journal*, *7*(4). https://doi.org/10.1007/s42452-025-06718-7

Mohapi, M., Sefadi, J. S., Mochane, M. J., Magagula, S. I., & Lebelo, K. (2020). Effect of LDHs and Other Clays on Polymer Composite in Adsorptive Removal of Contaminants: A Review. *Crystals*, *10*(11), 957. https://doi.org/10.3390/cryst10110957

Moreno-Rodríguez, D., Jankovič, Ľ., Scholtzová, E., & Tunega, D. (2021). Stability of Atrazine–Smectite Intercalates: Density Functional Theory and Experimental Study. *Minerals*, *11*(6), 554–554. https://doi.org/10.3390/min11060554

Murphy, O. P., Vashishtha, M., Palanisamy, P., & Kumar Kannuchamy, V. (2023). A Review on the Adsorption Isotherms and Design Calculations for the Optimization of Adsorbent Mass and Contact Time. *ACS Omega*, *8*(20), 17407–17430. https://doi.org/10.1021/acsomega.2c08155

Muthukkumaran, A., & Aravamudan, K. (2017). Combined Homogeneous Surface Diffusion Model – Design of experiments approach to optimize dye adsorption considering both equilibrium and kinetic aspects. *Journal of Environmental Management*, *204*, 424–435. https://doi.org/10.1016/j.jenvman.2017.09.010

Ngeno, E. C., Mbuci, K. E., Necibi, M. C., Shikuku, V. O., Olisah, C., Ongulu, R., Matovu, H., Ssebugere, P., Abushaban, A., & Sillanpää, M. (2022). Sustainable re-utilization of waste materials as adsorbents for water and wastewater treatment in Africa: Recent studies, research gaps, and way forward for emerging economies. *Environmental Advances*, *9*, 100282. https://doi.org/10.1016/j.envadv.2022.100282

Obayomi, O. V., Olawoyin, D. C., Oguntimehin, O., Mustapha, L. S., Kolade, S. O., Oladoye, P. O., Oh, S., & Kehinde Shola Obayomi. (2024). Exploring Emerging Water Treatment Technologies for the Removal of Microbial Pathogens. *Current Research in Biotechnology*, *8*, 100252–100252. https://doi.org/10.1016/j.crbiot.2024.100252

Osman, A. I., Ayati, A., Farghali, M., Krivoshapkin, P. V., Tanhaei, B., Karimi-Maleh, H., Krivoshapkina, E. F., Taheri, P., Tracey, C., Al-Fatesh, A. S., Ihara, I., Rooney, D., & Sillanpää, M. (2023). Advanced adsorbents for ibuprofen removal from aquatic environments: a review. *Environmental Chemistry Letters*. https://doi.org/10.1007/s10311-023-01647-6

Oyewo, O. A., Muliwa, A. M., Makgato, S. S., & Onwudiwe, D. C. (2024). Research progress on green adsorption process for water pollution control applications. *Hybrid Advances*, 100338. https://doi.org/10.1016/j.hybadv.2024.100338

Pandey, R., Pandey, L., Mishra, S. K., & Mishra, M. K. (2024, April 1). *Agrochemicals and Their Impact on Environment*. https://www.researchgate.net/publication/375485756_Agrochemicals_and_Their_Impact_on_Environment

Pangesti, G. G., Pandiangan, K. D., Simanjuntak, W., Sascori, S., & Rilyanti, M. (2021). Synthesis of zeolite-Y from rice husk silica and food grade aluminum foil using modified hydrothermal method. *Journal of Physics Conference Series*, *1751*, 012089–012089. https://doi.org/10.1088/1742-6596/1751/1/012089

Penn, C. J., Gonzalez, J. M., & Chagas, I. (2018). Investigation of Atrazine Sorption to Biochar With Titration Calorimetry and Flow-Through Analysis: Implications for Design of Pollution-Control Structures. *Frontiers in Chemistry*, *6*. https://doi.org/10.3389/fchem.2018.00307

Qiao, C., Zhang, Y., Zhu, Y., Cao, C., Bao, X., & Xu, J. (2015). One-step synthesis of zinc–cobalt layered double hydroxide (Zn–Co-LDH) nanosheets for high-efficiency oxygen evolution reaction. *Journal of Materials Chemistry A*, *3*(13), 6878–6883. https://doi.org/10.1039/c4ta06634k

Raheem, S. A., & Mohammed, A. A. (2025). Synthesis, characterization, and applications of layered double hydroxides nanocomposites for the adsorption of organic and inorganic contaminants from an aqueous solution: An overview. *Results in Surfaces and Interfaces*, *18*, 100386. https://doi.org/10.1016/j.rsurfi.2024.100386

Rea, G., Polticelli, F., Antonacci, A., Scognamiglio, V., Katiyar, P., Kulkarni, S. A., Johanningmeier, U., & Maria Teresa Giardi. (2009). Structure-based design of novel *Chlamydomonas reinhardtii* D1-D2

photosynthetic proteins for herbicide monitoring. *Protein Science*, *18*(10), 2139–2151. https://doi.org/10.1002/pro.228

Sahu, D., Pervez, S., Karbhal, I., Tamrakar, A., Mishra, A., Ranjan Verma, S., Manas Kanti Deb, Ghosh, K. K., Yasmeen Fatima Pervez, Kamlesh Shrivas, & Satnami, M. L. (2024). Applications of Different Adsorbent Materials for the Removal of Organic and Inorganic Contaminants from Water and Wastewater– A Review. *Desalination and Water Treatment*, *317*, 100253–100253. https://doi.org/10.1016/j.dwt.2024.100253

Sajid, M., & Basheer, C. (2016). Layered double hydroxides: Emerging sorbent materials for analytical extractions. *TrAC Trends in Analytical Chemistry*, *75*(1), 174–182. https://doi.org/10.1016/j.trac.2015.06.010

Sarkar, S., & Upadhyay, C. (2025). Layered double hydroxides for industrial wastewater remediation: A review. *Catalysis Today*, *445*(1), 115101. https://doi.org/10.1016/j.cattod.2024.115101

Satyam, S., & Patra, S. (2024). Innovations and challenges in adsorption-based wastewater remediation: A comprehensive review. *Heliyon*, *10*(9), e29573. https://doi.org/10.1016/j.heliyon.2024.e29573

Shahzad, A., Ullah, M. W., Ali, J., Aziz, K., Javed, M. A., Shi, Z., Manan, S., Ul-Islam, M., Nazar, M., & Yang, G. (2023). The versatility of nanocellulose, modification strategies, and its current progress in wastewater treatment and environmental remediation. *Science of the Total Environment*, *858*, 159937. https://doi.org/10.1016/j.scitotenv.2022.159937

Taylor, C. J., Pomberger, A., Felton, K. C., Grainger, R., Barecka, M., Chamberlain, T. W., Bourne, R. A., Johnson, C. N., & Lapkin, A. A. (2023). A Brief Introduction to Chemical Reaction Optimization. *Chemical Reviews*, *123*(6). https://doi.org/10.1021/acs.chemrev.2c00798

Torres-Castañón, L. A., Robledo-Peralta, A., Antileo, C., Silerio-Vázquez, F. de J., & Proal-Nájera, J. B. (2025). Sawdust-based adsorbents for water treatment: An assessment of their potential and challenges in heavy metal adsorption. *Journal of Hazardous Materials Advances*, *18*, 100758. https://doi.org/10.1016/j.hazadv.2025.100758

Trivedi, Y., Sharma, M., Mishra, R. K., Sharma, A., Joshi, J., Gupta, A. B., Achintya, B., Shah, K., & Vuppaladadiyamd, A. K. (2025). Biochar potential for pollutant removal during wastewater treatment: A comprehensive review of separation mechanisms, technological integration, and process analysis. *Desalination*, *600*, 118509. https://doi.org/10.1016/j.desal.2024.118509

Tucker-Quiñónez, A. M., Rivadeneira-Mendoza, B. F., Gorozabel-Mendoza, M. L., Pérez-Almeida, I. B., García-Guerrero, A. J., Dueñas-Rivadeneira, A. A., Yadav, K. K., Zambrano-Intriago, L. A., & Rodríguez-Díaz, J. M. (2025). Challenges and potential of layered double hydroxides as electrocatalytic materials for hydrogen production from water: A review of recent advances and applications. *Energy Nexus*, *17*, 100399. https://doi.org/10.1016/j.nexus.2025.100399

Vahdatkhah, A., Hosseinzadeh, H., Javanbakht, S., & Mohammadi, R. (2025). Fantastic composition of metal-organic frameworks with layered double hydroxides: Insights into synthesis, applications, and

synergistic effects. *Chemical Engineering Journal Advances*, *23*, 100768. https://doi.org/10.1016/j.ceja.2025.100768

Villar, M., Selvasembian, R., Giannakoudakis, D. A., Triantafyllidis, K. S., McKay, G., & Meili, L. (2022). Layered Double Hydroxides as Rising-Star Adsorbents for Water Purification: A Brief Discussion. *Molecules*, *27*(15), 4900–4900. https://doi.org/10.3390/molecules27154900

Wijitwongwan, R. (Ploy), Intasa-ard, S. (Grace), & Ogawa, M. (2019). Preparation of Layered Double Hydroxides toward Precisely Designed Hierarchical Organization. *ChemEngineering*, *3*(3), 68. https://doi.org/10.3390/chemengineering3030068

Zhang, Z., Tang, L., Luo, J., Tan, J., & Jiang, X. (2025). Comparative study of Mg/Al-LDH and Mg/Fe-LDH on adsorption and loss control of 2,4-dichlorophenoxyacetic acid. *Advanced Biotechnology*, *3*(1). https://doi.org/10.1007/s44307-024-00055-3